Master Thesis

Czech Technical University in Prague

F3

Faculty of Electrical Engineering
Department of Measurement

Flight Control Solutions Applied for Improving Vehicle Dynamics

Marek László

Supervisor: Ing. Tomáš Haniš, Ph.D.
Field of study: Cybernetics and Robotics
Subfield: Aerospace Systems
January 2019

MASTER'S THESIS ASSIGNMENT

I. Personal and study details

Student's name: **László Marek** Personal ID number: **461379**

Faculty / Institute: **Faculty of Electrical Engineering**

Department / Institute: **Department of Measurement**

Study program: **Cybernetics and Robotics**

Branch of study: **Aerospace Systems**

II. Master's thesis details

Master's thesis title in English:

Flight Control Solutions Applied for Improving Vehicle Dynamics

Master's thesis title in Czech:

Použití systémů řízení letu pro úpravu dynamiky pozemních vozidel

Guidelines:

The goal of the thesis is to investigate applicability of selected SAS (stability-augmentation-systems) architectures and related control design methodologies for drive stabilization of terrestrial vehicles. The long-time approved flight controls design and validation toolchain shall be emulated in a simplified manner (see details below) for the terrestrial vehicle case, to attract attention of industrial partners in the aerospace and automotive fields, and to identify specific promising topics for further research. Drive tests will be conducted in collaboration with the eForce FEE Prague formula student electric.
1. Get familiar with advanced actuating concepts for modern and upcoming cars (active differentials, torque vectoring, differential braking etc.).
2. Adopt and develop suitable simulation models using IPG Carmaker simulation environment.
3. Propose and realize a simulation platform.
4. Suggest suitable architectures for active vehicle control and parameterize the controllers for selected cases.
5. Validate the control solutions by simulations in MATLAB/Simulink.
6. Validate the control solutions on the simulation platform.
7. Verify one selected functionality in a drive test.

Bibliography / sources:

[1] Nelson: Flight stability and automatic control, McGraw-Hill Education 1997.
[2] Kiencke, Nielsen: Automotive Control Systems, Springer 2005.

Name and workplace of master's thesis supervisor:

Ing. Tomáš Haniš, Ph.D., Katedra řídicí techniky, CVUT - FEL

Name and workplace of second master's thesis supervisor or consultant:

Date of master's thesis assignment: **04.10.2018** Deadline for master's thesis submission: **15.01.2019**

Assignment valid until:
by the end of winter semester 2019/2020

Ing. Tomáš Haniš, Ph.D. Supervisor's signature	Head of department's signature	prof. Ing. Pavel Ripka, CSc. Dean's signature

III. Assignment receipt

The student acknowledges that the master's thesis is an individual work. The student must produce his thesis without the assistance of others, with the exception of provided consultations. Within the master's thesis, the author must state the names of consultants and include a list of references.

. _____
Date of assignment receipt

_____
Student's signature

Acknowledgements

I would like to express my gratitude to all lecturers who gave me the theoretical foundations during my master studies.

I would like to thank my supervisor Ing. Tomáš Haniš, Ph.D. for his valuable advises and evenings spent solving problems together. Secondly, I would like to thank doc. Ing. Martin Hromčík, Ph.D. for support and past projects that resulted in this work.

Great thanks also to formula student electric team eForce FEE Prague Formula for support and designing of winning vehicle without which this thesis would not have been possible. Namely, Bc. Patrik Bachan, Bc. Lukáš Hostačný, Ondřej Šereda, Bc. Radovan Juráš, Bc. Radek Štěpánek, Jakub Sedlář, Ing. Ondřej Hladík, Bc. Adam Čumrda and many more. I owe them a barrel of beer.

I would like to appreciate IPG Automotive for supporting the eForce formula student team and then my thesis with their IPG Carmaker software environment which I used for vehicle simulation and testing.

I also thank my family, girlfriend and friends for their support throughout my studies.

Poďakovanie

Chcel by som vyjadriť svoju vďačnosť všetkým prednášajúcim, vďaka ktorým som získal potrebné teoretické základy počas magisterského štúdia.

Rád by som poďakoval vedúcemu mojej diplomovej práce Ing. Tomášovi Hanišovi, Ph.D. za jeho cenné rady a večeri strávené riešením problémov. Tiež by som chcel poďakovať doc. Ing. Martinovi Hromčíkovi, Ph.D. za podporu a predošlé projekty, ktoré viedli k tejto práci.

Veľké poďakovanie patrí tiež tímu študentskej elektrickej formule eForce FEE Prague Formula za podporu a vývoj víťazného vozidla bez čoho by táto práca nemohla vzniknúť. Menovite sú to Bc. Patrik Bachan, Bc. Lukáš Hostačný, Ondřej Šereda, Bc. Radovan Juraš, Bc. Radek Štěpánek, Jakub Sedlář, Ing. Ondřej Hladík, Bc. Adam Čumrda a mnoho ďalších.

Tiež som vďačný firme IPG Automotive GmbH za poskytnutie simulačného softvéru IPG Carmaker, ktorý som používal pri vývoji a testovaní.

Ďalej ďakujem svojej rodine, priateľke a kamarátom za ich podporu počas môjho štúdia.

Declaration

I hereby declare that this master thesis was finished on my own and that I have cited all the used information sources in the list of references according to the *Methodical guideline on the observance of ethical principles in the preparation of university graduate thesis.*

Prehlásenie

Prehlasujem, že som predloženú diplomovú prácu vypracoval samostatne a že som uviedol všetky použité informačné zdroje v súlade s *Metodickým pokynem o dodržování etických principů při přípravě vysokoškolských závěrečných prací.*

In Prague/V Prahe, 7. 1. 2019

Abstract

Development of electric vehicles gives new possibilities for vehicle dynamics control by the introduction of the individual-wheel driven platforms. A fast response time of electric powertrain also allows for further progress in existing solutions.

The goal of this thesis is to improve electric formula student handling characteristics with the introduction of active torque vectoring and additional control systems. Namely yaw rate tracking and yaw damper were implemented. The system is developed using a model-based design approach and tested by virtual test drives, restbus simulation, and experimental drive tests.

Keywords:
vehicle dynamics, vehicle stability, electric vehicles control systems, torque vectoring system, driver assistance system, oversteer, understeer, IPG Carmaker, 4WD, formula student electric, vehicle dynamics tests, restbus, model-based design, slip ratio control system, traction control

Supervisor:
Ing. Tomáš Haniš, Ph.D.
České vysoké učení technické
v Praze,
Fakulta elektrotechnická,
Katedra řídicí techniky - K13135,
Karlovo náměstí 13,
12135 Praha 2

Abstrakt

Súčasný vývoj elektrických vozidiel prináša nové možnosti ohľadom riadenia dynamiky vozidla vďaka prínosom individuálneho pohonu kolies. Rýchla odozva elektrického pohonu dáva nové možnosti vývoja už existujúcim systémom.

Cieľom tejto práce je vylepšenie charakteristík jazdnej dynamiky študentskej elektrickej formule použitím aktívneho prerozdeľovania hnacieho momentu a s pomocou ďalších riadiacích systémov. Implementovaný bol tlmič uhlovej rýchlosti zatáčania a riadenie na referenčnú uhlovú rýchlosť zatáčania. Systém bol vyvinutý prístupom model-based designu a overený virtuálnymi jazdnými skúškami, restbus simuláciou a experimentálnymi jazdnými skúškami.

Kľúčové slová:
dynamika vozidla, stabilita vozidla, elektrické vozidlá, riadiace systémy, systém prerozdeľovania hnacieho momentu, pretáčavosť, nedotáčavosť, IPG Carmaker, 4WD, študentská elektrická formula, testy dynamiky vozidla, restbus, model-based design, riadenie preklzu, trakčná kontrola

Preklad názvu:
Použitie systému riadenia letu pre úpravu dynamiky pozemných vozidel

Contents

Acronyms

4WD Four Wheel Drive

ABS Anti-lock Braking System

CAN Controller Area Network

CAS Control Augmentation System

CCP CAN Calibration Protocol

CoG Center of Gravity

CoP Center of Pressure

CPI Contact Patch Interface

CM4SL Carmaker for SimuLink

DIL Driver-In-the-Loop

ECU Electronic Control Unit

EKF Extended Kalman filter

ESC Electronic Stability Control

FR Front Right

FL Front Left

KML Keyhole Markup Language

GNSS Global navigation satellite system

IMU Inertial Measurement Unit

INS Inertial Navigation System

ISO International Organization for Standardization

PC Personal Computer

PCB Printed Circuit Board

PID Proportional, Integral and Derivative

RR Rear Right

RL Rear Left

SAE Society of Automotive Engineers

SAS Stability Augmentation System

SIL Software-In-the-Loop

STI Standard Tire Interface

TCL Tool Command Language

TCS Traction Control System

TRQ Torque

TV Torque Vectoring

TYDEX The Tyre Data Exchange Format

VDCU Vehicle Dynamics Control Unit

List of symbols

a - acceleration

a_1 - distance between CoG and front axle

a_2 - distance between CoG and rear axle

a_{CL1} - distance between CoP and front axle

a_{CL2} - distance between CoP and rear axle

α - tire side-slip angle

β - vehicle side-slip angle

C_L - aerodynamic lift force

δ - wheel angle

η - slip ratio

i - transmission gear ratio

F_x - longitudinal force

F_y - lateral force

F_z - normal load

I_z - moment of inertia about the z-axis

l - length of the vehicle

m - vehicle mass

μ - friction coefficient

r - vehicle tire diameter

R - cornering radius

T_M - motor torque

Trq - overall desired torque

Trq_{MFR} - front right motor torque

Trq_{MFL} - front left motor torque

Trq_{MRR} - rear right motor torque

Trq_{MRL} - rear left motor torque

v - velocity of vehicle CoG

v_x - longitudinal velocity

v_y - lateral velocity

ψ - vehicle yaw

$\dot{\psi}$ - vehicle yaw rate

Chapter 1

Introduction

Automotive industry is getting safer due to developments in the domain of chassis, Electronic Stability Control (ESC) or by active avoidance systems. The ESC system helps the driver to maintain the control even in situations where it would be normally lost. The aim of this thesis is to implement a lateral control strategy to improve the performance of competition vehicle in means of:

- Increased lateral acceleration.
- More linear steering response.
- Increased stability in the sense of yaw rate disturbance rejection.

Cornering behavior of vehicle can be characterized by understeering gradient which is shown on fig. 1.1 and its equation 1.1. The gradient describes the effect of steering angle changes on lateral acceleration. For a neutral vehicle, the characteristics should be linear. It is not possible and not beneficial for a vehicle without feedback control system due to its possible instability. Therefore, all vehicles are developed as understeer (stable). It is possible to actively manipulate the vehicle handling characteristics by the implementation of Torque Vectoring system (TV) that utilizes the electric powertrain to generate a yaw torque on a vehicle body.

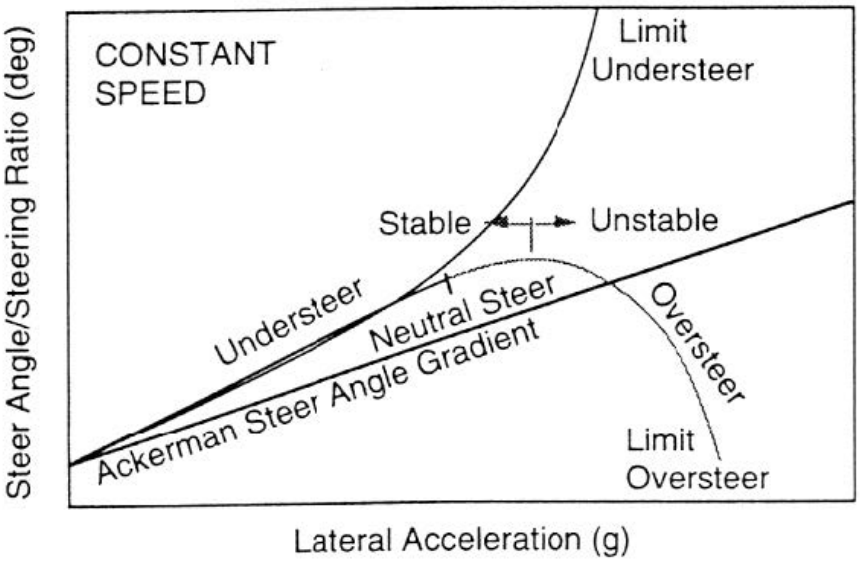

Figure 1.1: Vehicle handling and understeering gradient [7].

$$K = \frac{\partial \delta}{\partial a_y} \tag{1.1}$$

Several definitions of vehicle static characteristics and vehicle dynamics maneuver exists. According to the most common definition, the vehicle has understeer static characteristics, or it is in understeered maneuver, when slip angle on the front axle is higher than one on the rear axle, or it has oversteered static characteristics, or is in oversteered maneuver when slip angle on the rear axle is developing faster than the one on the front axle. The alternative definition says that the static characteristics of a vehicle are understeered when the understeering gradient is positive and oversteered when the understeering gradient is negative and neutral otherwise [15].
Extreme examples of vehicle handling during cornering are shown on fig. 1.2.

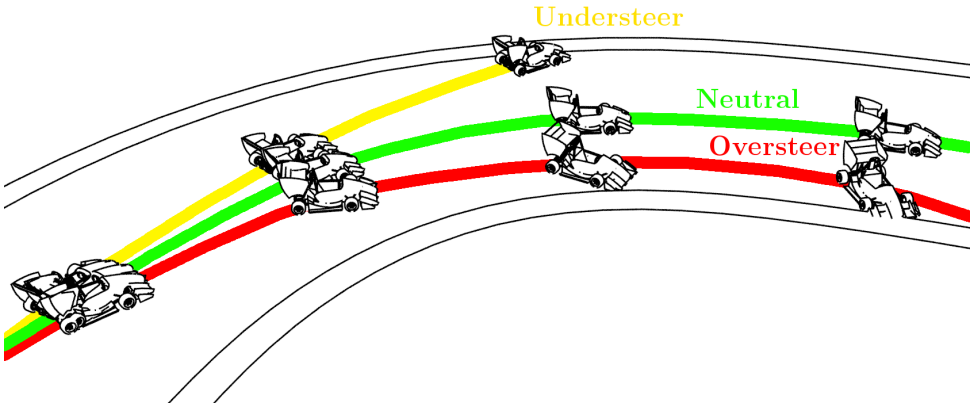

Figure 1.2: Basic types of vehicle handling. Illustration of understeering, oversteering and neutral steering.

Current systems were mainly developed for the safety reasons and mostly for combustion cars. The combustion engines dynamic response is slower by orders compared to electric motors and is also limited by environmental factors. On top of that, there is mostly only one combustion engine in a vehicle. Therefore, the feasible option to create yaw torque is limited to applying braking actions asymmetrically. This type of vehicle dynamics control dissipates energy into heat, and the dynamic response of brake is still significantly slower compared to electric motors. Limitations of the combustion system are obvious therefore the systems as Electronic Stability Control (ESC) [22] are mainly focused on safety by trying to force the vehicle back to the linear regime when non-linearity (high side slip angle) occurs. This greatly increases controllability, but performance might suffer. Robustness of the system is important as passenger cars are driven under different road conditions, vehicle passenger and cargo configuration.

In the last decade, there were significant advances within the development of electric cars leading to their more common use. Standardly the electric powertrain consists of two to four e-motors, and therefore the vehicle has independent wheel drive which is suitable for generating yaw torque which leads to a system called active torque vectoring [19]. Rimac Concept One uses advanced all wheel torque vectoring system called RAWTV[1] that covers the functionalities of traditional systems. Their custom made high-performance powertrain uses four e-motors. It was presented that the driver can easily adjust the torque vectoring settings.

Formula SAE is an automotive student competition. It was started in the USA and focuses on the education of future automotive engineers. The competition consists of static and dynamic disciplines. Judges rate presentation skills, theoretical and practical knowledge of the vehicle. Vehicle performance is evaluated by lap times. The composition of all disciplines gives the final

[1]Rimac Concept One RAWTV `http://www.rimac-automobili.com/en/latest/news/rimac-all-wheel-torque-vectoring/`

result. Improving the lateral dynamics of the vehicle is, therefore, crucial for good ranking.

I was part of an electric formula SAE project, eForce FEE Prague Formula[5] which is shown on fig. 1.4 and 1.3. My responsibility was the development of vehicle dynamics control systems.

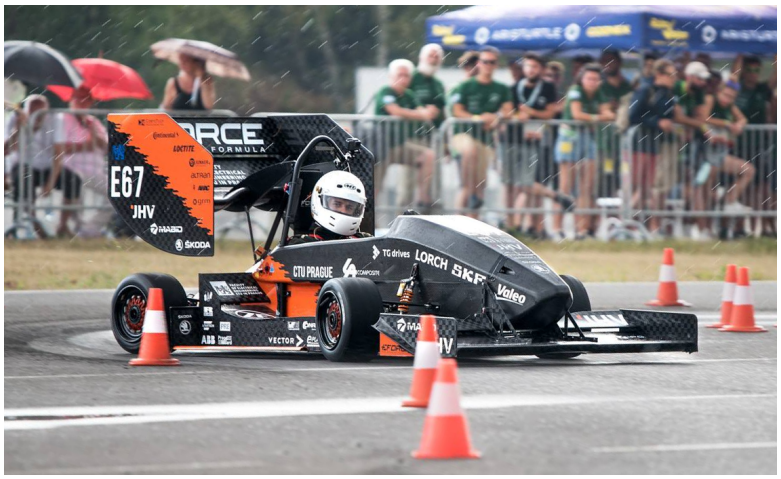

Figure 1.3: EForce FEE Prague Formula SAE during race. Me driving the electric formula SAE at Formula SAE Czech Republic competition in 2017/2018.

Figure 1.4: EForce FEE Prague Formula SAE team 2017/2018. Team photo during Netherlands formula SAE competition.

Presented thesis is a result of my work on formula student. There are limitations due to safety which is not considered in this thesis as the aim is on a prototype vehicle.

Chapter 2

Aerospace to automotive technology transfer

Advanced aerospace systems were in development since the 1940s. Due to army involvement and space race, the systems advanced quickly. Initially, only Stability Augmentation Systems (SAS) [12] were used. These operated existing mechanical links and only increased damping characteristics while the system opposed pilot inputs. Typically had low control authority and the aircraft response was decreased due to damping. Yaw, pitch and roll dampers were used to increase stability. Control Augmentation Systems (CAS) [12] were first feedback control systems introduced to improve the vehicle handling further with higher control authority. By implementing the fly-by-wire system the control authority might be fully taken. Many fighter jets of later generations use this system together with more advanced technology as thrust vectoring .etc. Airbus is known to be first who adopted the fly-by-wire system for public transportation.

In history, some researchers made their findings as in aerospace also in the automotive industry which shows the similarity between the industries. One of these examples is W.F. Milliken.

As can be seen on fig. 2.1 there is a great similarity between the lift coefficient and vehicle tire force characteristics. Especially the airplane longitudinal characteristics consisting of phugoid and short period modes as can be seen on fig. 2.2(more details in [12]) is similar to the lateral car characteristics. The main difference is that car has critical speed above which it seems to be unstable while airplane has a critical speed below which it stalls and is therefore unstable.

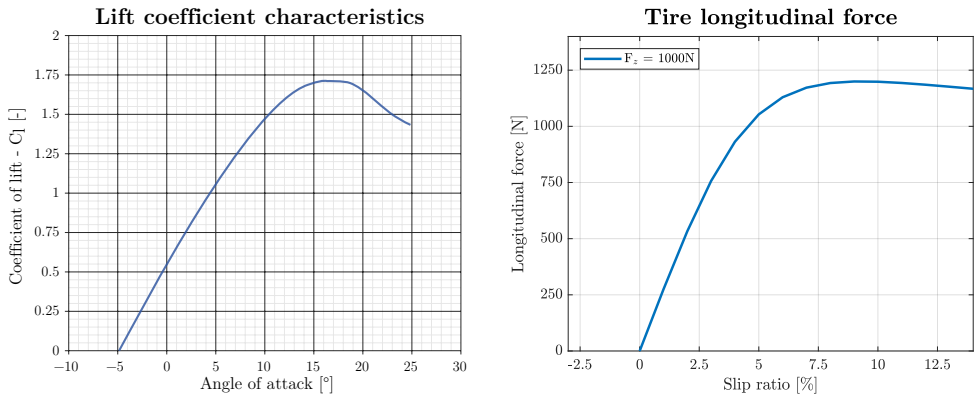

Figure 2.1: Comparison between flight and vehicle dynamics. There is obvious similarity between tire and wing characteristics. More details on lift coefficient curve are in [3]

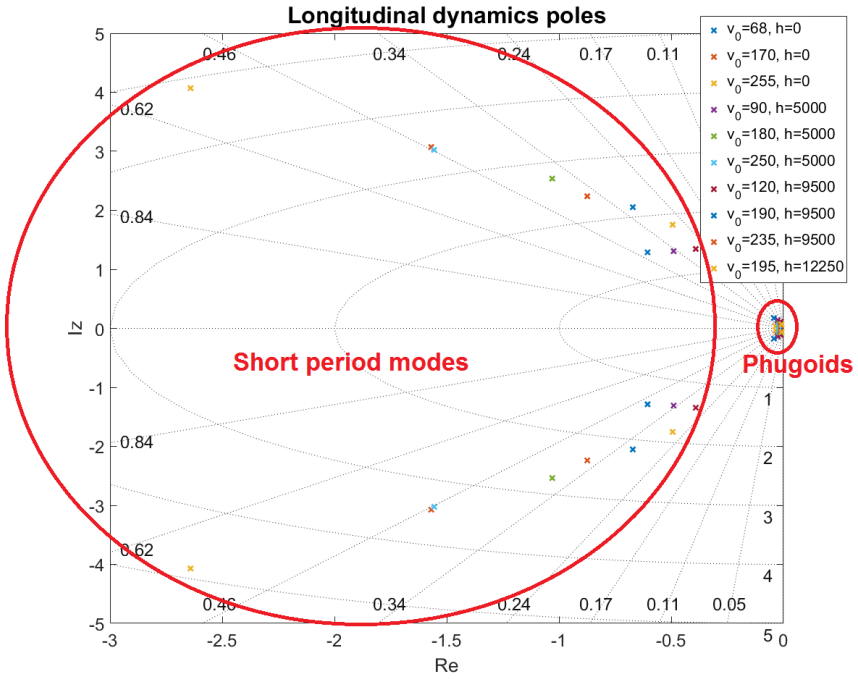

Figure 2.2: Plane longitudinal dynamics modes in flight envelope.

With SAS, the short period mode is dampen by use of pitch damper as seen on fig. 2.3. Pitch damper is realized as direct feedback from pitch rate to vertical control surface servo input.

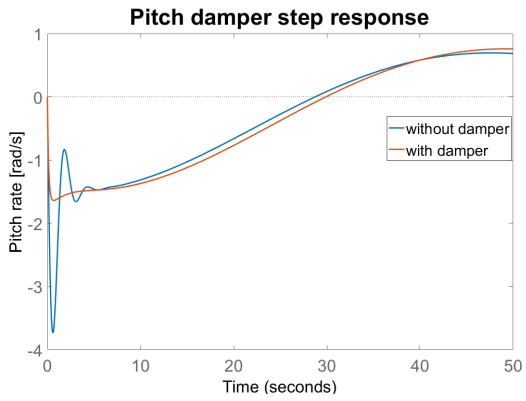

Figure 2.3: Elevator step response with and without pitch damper.

Due to these similarities a simple implementation of pitch damper should increase the damping factor of vehicle lateral dynamics response.

Chapter 3

Vehicle dynamics modeling

3.1 Introduction to vehicle modeling

The vehicle longitudinal and lateral modes could be considered as decoupled if the tire slip angles and slip ratios are small enough and the vehicle is not driving on traction limits. Lateral model and longitudinal models might be then developed independently.

For a control design, a linear model should be considered. A linearized single-track constant speed model is used for lateral dynamics analyses. Twin track model can be used if the single track model is not enough. Rigid or even flexible multibody models might be used for controller validation, virtual test driving or further research.

A single track nonlinear model and multibody model were extensively used through the whole design process. This was decided because the performance vehicle drives at limits and uses aerodynamic devices making linear analysis possible but not very practical given the tight time constraints for the design and high amount of work concerning the implementation of the software using new model-based design approach.

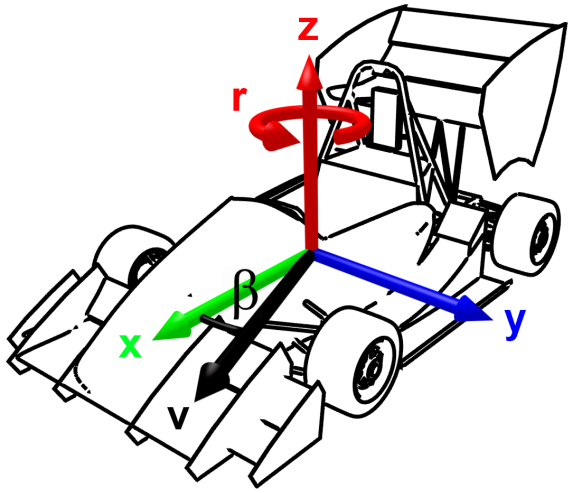

Figure 3.1: Vehicle coordinate system. Coordinate system used within models and measurements.

3.2 Tire models

Tire is the only part of the vehicle that has direct interaction with road surface in its contact patch. A significant amount of work in performance vehicle design is dedicated to keeping the tire in the best possible shape with the most contact possible. Therefore a good tire model is crucial for the success of the whole vehicle design. Description with mathematical models of the tire can be found in [16].

Three different mechanisms are generating the tire force: adhesion, deformation, tearing [14]. Tire generates traction forces mainly dependent on normal load force, slip angle, slip ratio. As seen on fig. 3.2 these forces are limited by Kamm's circle of forces. Absolute force value is therefore bounded, and the vehicle is unable to accelerate longitudinally and laterally in a high rate at the same time as is shown by equation 3.1.

$$\mu F_z = \sqrt{F_x^2 + F_y^2}. \tag{3.1}$$

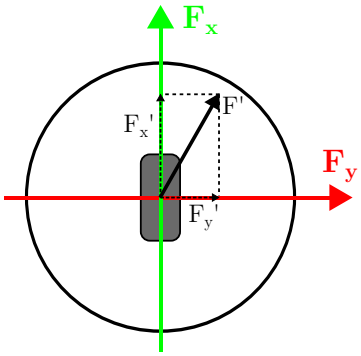

Figure 3.2: Kamm's circle. Traction forces are bounded.

Tire coordinate system used is defined in fig. 3.3.
There is no universally agreed definition of tire slip ratio η equation therefore we use SAE J670 [18] notation 3.2 that is used in IPG Carmaker [2]. Side slip angle α equation is 3.3.

$$\eta = \left(\frac{\omega_w R_c}{v_x} - 1 \right) \cdot 100 \tag{3.2}$$

$$\alpha = arctan\left(\frac{v_y}{|v_x|} \right) \tag{3.3}$$

Tire models are using Contact Patch Interface (CPI) or Standard Tire Interface (STI). First mentioned calculates the forces and torques in contact patch while later describes the whole tire behavior with its vertical dynamics by outputting forces and torques in the wheel carrier frame.

Many of the tire models do not accommodate for tire thermal behavior. Tire measurements are showing as challenging as the grip is greatly affected by temperature and wear. There is a deviation with models that do not account for heating, especially for a race vehicle. Some situations like as driving through dirt are even more complicated to simulate. There are many tire models with different uses. Only a few of those models are discussed in this section.

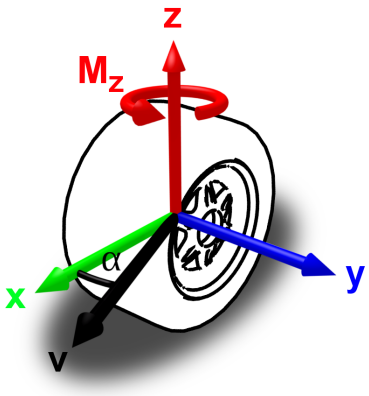

Figure 3.3: Tire coordinate system. Coordinate system used within tire models.

3.2.1 Pacejka Magic Formula

Pacejka Magic formula is well known empirical tire model in the industry with the calculation of forces and torques for contact patch (CPI). The model uses a fit of mathematical curves with parameters known as shape factors and two-dimensional slip inputs. Factors are D,B,C,E and are further detailed in [16]. These slip curves were initially defined by Hans Bastiaan Pacejka [13] and the parameterizing shape factors were named by their observed function in the characteristics. Pacejka later defined many more tire parameters that have dependencies and together form the shape factors. This tire model is easily fitted to measurements, stored and used for real-time computations. The used tire characteristics can be seen on fig. 3.4. Longitudinal force is defined by equation (3.4a) while lateral force is defined by equation (3.4b) and aligning moment by equation (3.4c). It can be seen that these equations are very similar and therefore makes a significant difference in parametrization. By introducing newer equations with new parameters like the tire inclination angle, pressure and many more effects can be modeled. For a single track model, a simple Pacejka model is used. Problem with it is that it gets unstable while driving at a lower speed due to slip calculation problems. The model is not suitable for slow speed and standstill simulations.

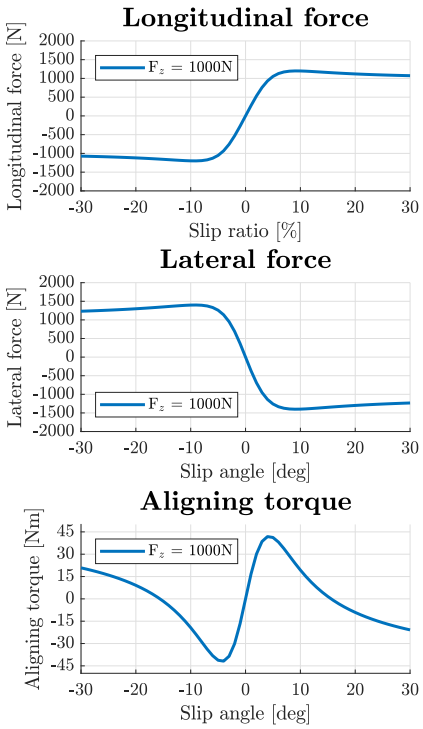

Figure 3.4: Tire model. Tire characteristics using Pacejka's Magic Formula.

$$F_x = F_z D_x sin(C_x arctan(B_x \eta - E_x(B_x \alpha - arctan(B_x \eta)))), \tag{3.4a}$$
$$F_y = F_z D_y sin(C_y arctan(B_y \alpha - E_y(B_y \alpha - arctan(B_y \alpha)))), \tag{3.4b}$$
$$M_z = F_z D_z sin(C_z arctan(B_z \alpha - E_z(B_z \alpha - arctan(B_z \alpha)))). \tag{3.4c}$$

3.2.2 Brush tire model

A physical tire model that models the tire contact patch with small brushes with defined length and stiffness as is described in [14]. Calculation of forces and torques is done for contact patch (CPI). This tire model needs more resources for computation, therefore, is not suitable for real-time models. It still uses simplifications of the contact patch physics.

3.2.3 TMeasy tire model

Semi-physical tire model developed mainly for truck tires but found use in automotive industry [17]. The model supports STI. A skilled engineer can parametrize the model as it has a physical basis. Uses discretized contact

patch with 3D slip approach. Automatically combines longitudinal and lateral dynamics. Has smooth transition from standstill to normal driving. Therefore this model is suitable for all driving situations even for parking and standstill [17].

3.2.4 TYDEX tire data format

The Tyre Data Exchange Format (TYDEX)[21] was defined to standardize the tire modeling in the industry. TYDEX tire calculates the forces and torques relative to wheel carrier (STI). It is easy to parametrize as inputs are lines of data similar to tire measurement.

For IPG Carmaker[1] a TYDEX model was used because of its easy parametrization and expandability. Although the format implementations by different companies are not always compatible.

3.3 Vehicle dynamics models

3.3.1 Kinematic vehicle model

Kinematic model is simple and yields excellent results only with small slip angles therefore at low speed. Can be assumed that the steering angle is average of the two front wheels steering angles. Instantaneous center of rotation is defined by the crossing of all wheels axis so always lays on an axis of rear axle which leads to a very simple solution. The derivation of the kinematic model is in [10]. Using goniometric to describe the model.

$$\tan(\delta) = \frac{w_b}{R}, \tag{3.5}$$

Cornering radius is obtained by

$$R = \frac{w_b}{\tan(\delta)}, \tag{3.6}$$

With knowledge of speed a yaw rate can be calculated as follows

$$\dot{\psi} = \frac{v}{R} = \frac{v \tan(\delta)}{w_b}. \tag{3.7}$$

For a better approximation, a mass, aerodynamics lift force and tires Kamm's circle can be implemented as a limitation factor for the lateral dynamics.

[1] IPG AUTOMOTIVE GmbH. `www.ipg.com`

3.3.2 Single track vehicle model

By reducing each axle right and left wheel to a single central wheel a single track [16] or sometimes referred to as bicycle model is obtained. Single-track model is simple and captures the dominant vehicle dynamics by use of slip angle and tire models. Linear single track model is used for controller design. The non-linear constant speed single-track model is used as yaw rate reference for yaw rate tracking control. Special care was taken during implementation and parametrization to prevent instability from occurring. To reassemble a formula student car an aerodynamic lift force was introduced to the model. Results of the model experimental validation are shown in section 3.4.

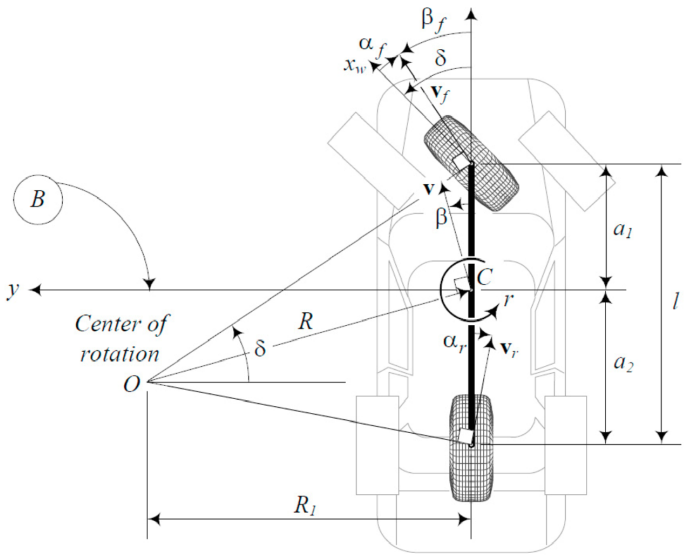

Figure 3.5: Single track vehicle model. Tire forces are defining the center of rotation. For low speed (small dynamic forces) the model acts as a kinematic model with center of rotation inline with a rear axle. The figure is adopted from [11].

$$\dot{\beta} = -\dot{\psi} + \frac{1}{mv}(\cos\beta(F_{yr} + \cos\delta F_{yf}) - \sin\beta(F_{xr} - \sin\delta F_{yf})), \tag{3.8a}$$

$$\dot{v} = \frac{1}{m}(\sin\beta(F_{yr} + \cos\delta F_{yf}) + \cos\beta(F_{xr} - \sin\delta F_{y}f)), \tag{3.8b}$$

$$\ddot{\psi} = \frac{1}{I_z}(a_1\cos\delta F_{yf} - a_2 F_{yr}). \tag{3.8c}$$

Tire normal forces equations with arms a_{1CL}, a_{2CL} are defining the Center of Pressure (CoP) [3] seen in equation 3.11a and equation 3.11b. Together

with slip angle equations 3.9a and 3.9b are used as inputs to tire model.

$$\alpha_f = \delta - \arctan\left(\frac{v\sin\beta + a_1\dot{\psi}}{v\cos\beta}\right), \tag{3.9a}$$

$$\alpha_r = -\arctan\left(\frac{v\sin\beta - a_2\dot{\psi}}{v\cos\beta}\right). \tag{3.9b}$$

$$F_{zf} = mg\left(\frac{a_2}{a_1+a_2}\right) - \frac{1}{2}\rho v^2 S C_L\left(\frac{a_{CL2}}{a_{CL1}+a_{CL2}}\right), \tag{3.10a}$$

$$F_{zr} = mg\left(\frac{a_1}{a_1+a_2}\right) - \frac{1}{2}\rho v^2 S C_L\left(\frac{a_{CL1}}{a_{CL1}+a_{CL2}}\right), \tag{3.10b}$$

$$F_{zf} = mg\left(\frac{a_2}{a_1+a_2}\right) - \frac{1}{2}\rho v^2 S C_L\left(\frac{a_{CL2}}{a_{CL1}+a_{CL2}}\right), \tag{3.11a}$$

$$F_{zr} = mg\left(\frac{a_1}{a_1+a_2}\right) - \frac{1}{2}\rho v^2 S C_L\left(\frac{a_{CL1}}{a_{CL1}+a_{CL2}}\right), \tag{3.11b}$$

Calculation of yaw torque created by single motor torque is presented in following equations 3.12a, 3.12b, 3.12c. A calculation of tractive force is performed in equation 3.12a using the transmission and tire radius parameters. In equation 3.12b a perpendicular force to axis that connects Center of Gravity (CG) and wheel is calculated. This force is transformed to torque by knowledge of wheel distance to the center of gravity. Calculated yaw torque is a single motor contribution.

$$F_x = \frac{T_M i}{r} \tag{3.12a}$$

$$F_{Tz} = F_x \sin(\arctan\left(\frac{T}{2a}\right)) \tag{3.12b}$$

$$T_z = F_{Tz}\sqrt{a^2 + \left(\frac{T}{2}\right)^2} \tag{3.12c}$$

3.3.3 Multibody vehicle model - IPG Carmaker

In a later stage of design and testing, a higher fidelity model is beneficial. Using the IPG Carmaker simulation environment for virtual test driving with

multibody model parametrized as seen on fig. 3.6. In the beginning, many example scenarios were tested to understand the IPG possibilities.

The vehicle definition is highly modular. Vehicle model structure can be set, and each system model can be adjusted or replaced by custom one. Suspension kinematics is defined and simulated in IPG Kinematics tool, and then a compiled version is used for real-time computation. The vehicle has a structure of controllers that can be overwritten. For vehicle dynamics control a general powertrain control unit was set from "Electrical" to Carmaker For Simulink ("CM4SL"). Information about used vehicle type, road geometry, maneuver, the driver, etc. is stored in a test run file. There are also many visualization possibilities as graphs are synchronized with the visualization, therefore, the analysis is convenient. A simple building segment or a Keyhole Markup language (KML) can be used to define a road geometry in the scenario editor. A route, road properties, and objects might be added to the scenario. Using a test manager, it is possible to define a whole test runs with evaluated outputs saved into a results file. Vehicle parameters can be changed for each of the test cases.

By using an IPG Driver, a vehicle can be driven reliably on a track. To compare the vehicle models, there is a possibility to create a document of vehicle characteristics. Pacejka Magic Formula, TYDEX and TameTire models are supported. The later models tire thermal behavior. We use TYDEX as explained in section 3.2.4. IPG Carmaker supports virtual sensors definition. These sensors might measure the physical quantity with respect to their position on a vehicle. The visualization module of IPG Movie is able to use custom made (.obj) models. By use of Tool Command Language (TCL), it is possible to add an interactive animation as animated torque input from Simulink which can be seen on fig. 3.7.

Multibody model is a good fit of the real vehicle as seen experimentally validated in section 3.4. It has an advantage of simulating more than four hundred vehicle signals that are sometimes very hard to measure in a real vehicle. The model can also be used to validate the state estimators as virtual sensors are configurable.

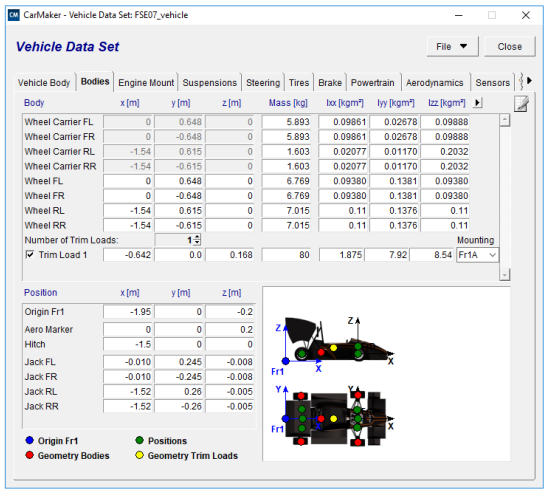

Figure 3.6: IPG Carmaker model parameters. Mass and inertia tensors are defined for rigid bodies. Other parameters are set under different configuration tabs.

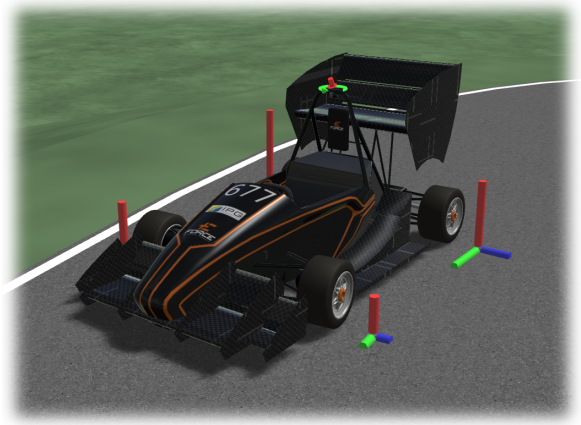

Figure 3.7: IPG Carmaker multibody vehicle model. Developed IPG Carmaker visualization model. Yaw torque and aerodynamic forces visualization was developed and can be seen at vehicles roll hoop.

3.4 Experimental model validation

To validate the models, test data were composed of selected maneuvers acquired by test driving. Steering and speed were used as input to the simulated models. On fig. 3.8 a whole composed test data can be seen. The models are stable and have a good fit to the actual measured data. In some cases, there is a small bias in the data and measured lateral acceleration is

overshooting due to the positioning of the IMU sensor near the front axle of the vehicle.

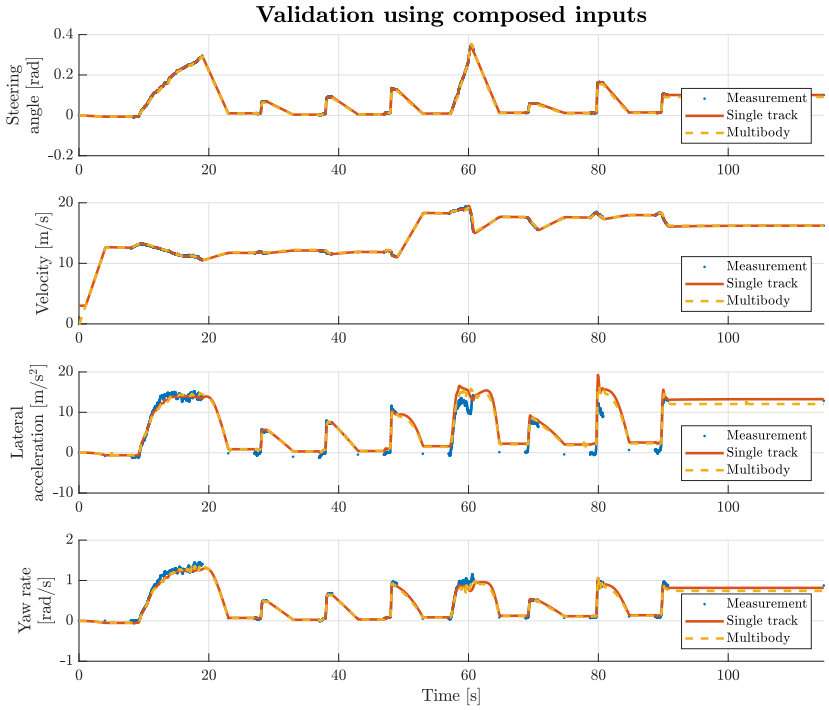

Figure 3.8: Validation of torque vectoring. Comparison of vehicle models. Inputs were composed from selected input signals that were measured on the test day.

By use of ramp steering, a steady state cornering can be evaluated. It is complicated to obtain a good quality measurement as ramp steering requires a significant free space of good quality tarmac. A seen on fig. 3.9 the models have a good fit. By replacing the time dependency by lateral acceleration, an understeering gradient can be seen on fig. 3.10.

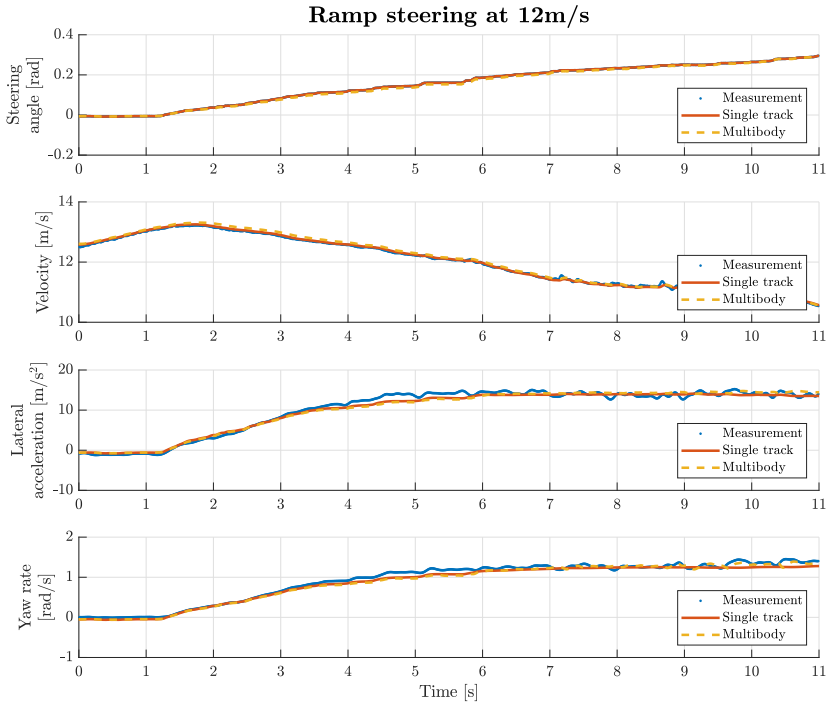

Figure 3.9: Validation of models by ramp steering. Ramp steering response in time for models used in design process.

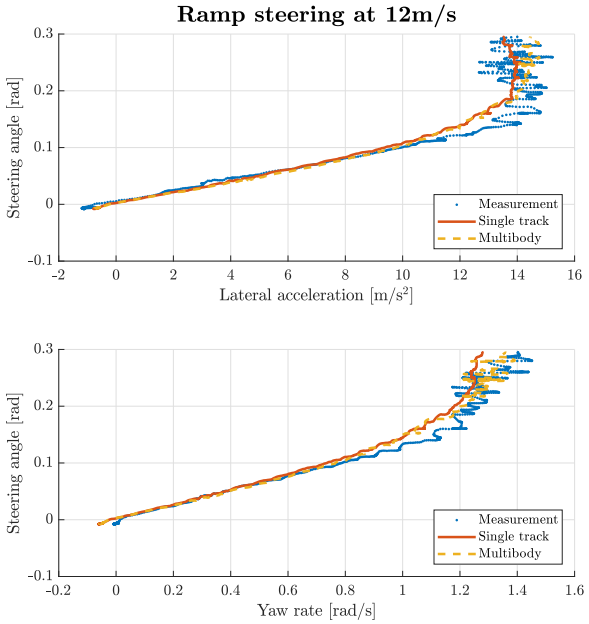

Figure 3.10: Ramp steering response. Understeering gradient (top) and yaw rate response (bottom) is shown.

Finally the transient dynamics is validated using a step steer input as seen on fig. 3.11. Measured lateral acceleration slightly leads and overshoots

probably due to the fact that IMU was not positioned in the center of rotation.

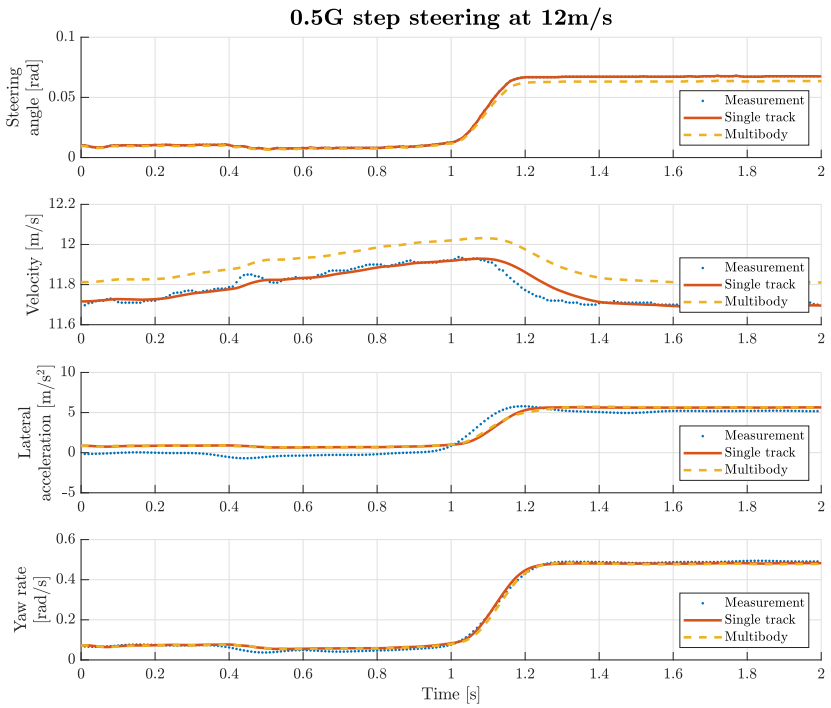

Figure 3.11: Validation of models by step steering. Step steering response in time for models used in design process.

Chapter 4

Torque vectoring control system development

4.1 Introduction

Open-loop torque vectoring also called an electronic differential was used in formula SAE with great success for years. Closed loop torque vectoring is based on a similar concept using the same torque distribution algorithm, and because of that, it is possible to switch between the algorithms.

The main idea of the torque vectoring described in the chapter 1 is to modify lateral vehicle dynamics by the introduction of yaw torque. The goal is to have neutral vehicle response and as linear behavior as possible with increased maximum lateral acceleration. It will make the vehicle more agile and stable and therefore more predictable to drive. This section deals with the implementation of the designed torque vectoring algorithms into the formula SAE electric four wheels driven vehicle. Torque vectoring is restricted by the rules [1]. A simple redistribution of the driver requested torque would not yield good results. Therefore, asymmetrical torque distribution creating yaw torque independent of torque request is used. Authority of yaw control is therefore high and equivalent under most of the circumstances.

Due to the powertrain limitation, it was not possible to use regenerative braking for the vehicle during real drive tests. A principle of yaw torque creation is shown in fig. 4.1.

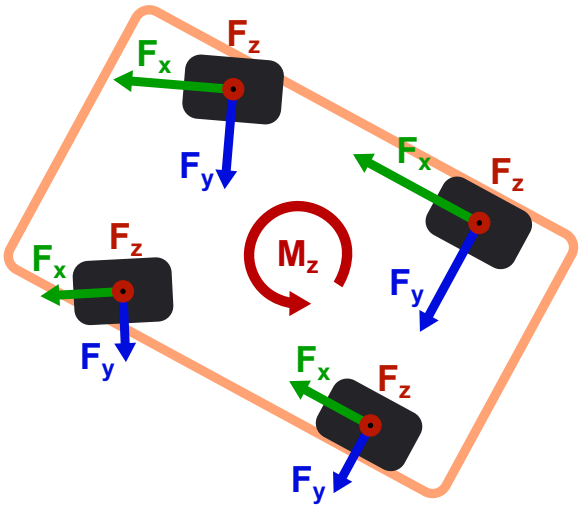

Figure 4.1: Illustration of torque vectoring. Yaw torque is created by redistribution of motor torques.

Available sensors for vehicle dynamics controls:

- 2x rear wheel speed sensors.
- 4x motor speed sensors.
- Accelerator pedal position sensor.
- Steering wheel angle sensor.
- Brake pressure sensor providing a pressure of front and rear brake circuit.
- Inertial Measurement Sensor (IMU) providing six degrees of freedom measurement.

4.2 Model-based design

The complex nature of designing a control unit software with many control subsystems under continuous development can be simplified by the use of a model-based design approach as described in [4]. The design takes place in a graphical programming environment of Simulink, and the resultant C code is generated using Embedded Coder and deployed to the Electronic Control Unit (ECU). Before integration, all systems are separately tested using offline simulations with plant models. Furthermore, a real-time virtual test driving is possible by replacing the vehicle network CAN bus interfaces with IPG

Carmaker interfaces. A suitable model architecture was designed to make these steps possible.

Presented VDCU hardware was also developed, but the design process is not in the scope of the thesis.

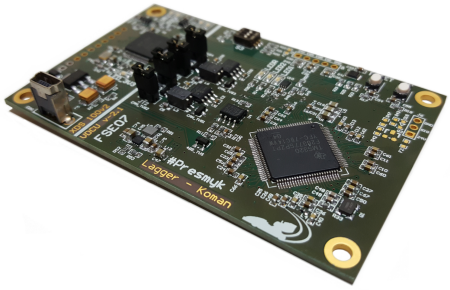

Figure 4.2: VDCU PCB. Custom made PCB of VDCU that is programmed using Simulink Embedded Coder and runs the software vehicles dynamics controls software.

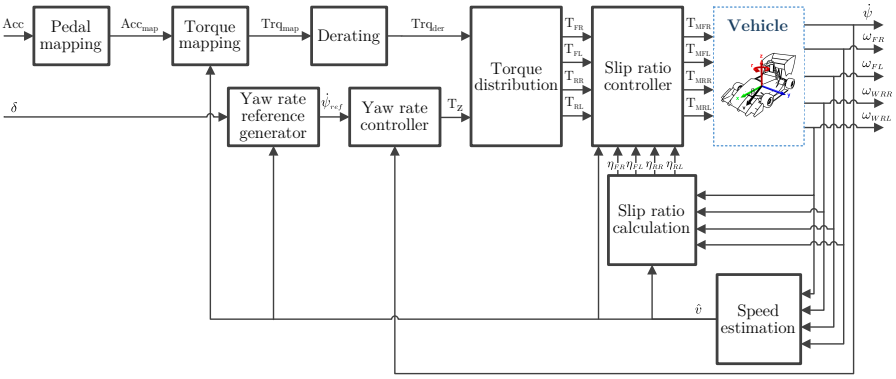

Figure 4.3: Yaw rate tracking control scheme overview. The path of driver inputs to actual motor torque command is shown in this scheme.

4.3 Speed estimation

The estimation of the vehicle center of gravity speed is crucial for maintaining a high control quality of speed controllers. It could be a separate topic with the state of art estimators implementing sensor fusion using Extended Kalman Filter (EKF) with great results. Described in 4.1 Velocity and positional measurements were not provided.

Due to the use in slip ratio control, these requirements need to be met:

- Estimated speed should not exceed the actual speed in the long term.
- Estimated speed should have a small deviation to actual speed.

While the estimate would exceed the actual speed a slip ratio controller would allow excessive slippage with a possible negative effect on vehicle stability.

Front motors of the used vehicle are less powerful, and their slippage is therefore less likely.

Two algorithms are proposed for the estimation:

- Averaging the wheel speeds.
- Using minimum wheel speed.

The advantage of using averaging is that the speed of the center of the front axle is estimated. The disadvantage is that during excessive wheel slippage the estimated speed significantly exceeds the actual speed. This problem is solved by using minimum wheel speed. Combination of the algorithms takes the best of both. Depending on the speed difference across wheels a different weighting is used. Final speed estimate is then composed of weighting average and minimum algorithms. Good results are achieved by averaging while the difference between wheel speeds is small. The minimum algorithm gives better result while one wheel is excessively slipping. This algorithm is far from the ideal but is less complex and reliable. Stopping one of the wheels (possibly by locking it during braking maneuver) would result in a zero estimated speed output which is incorrect, but the resultant vehicle controller behavior is safe.

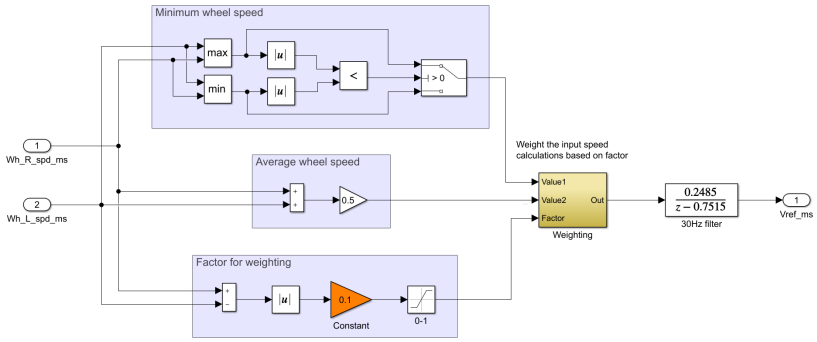

Figure 4.4: Speed estimator implementation. Software implementation of vehicle reference speed estimator in Simulink by weighting between minimum and average of wheel speeds.

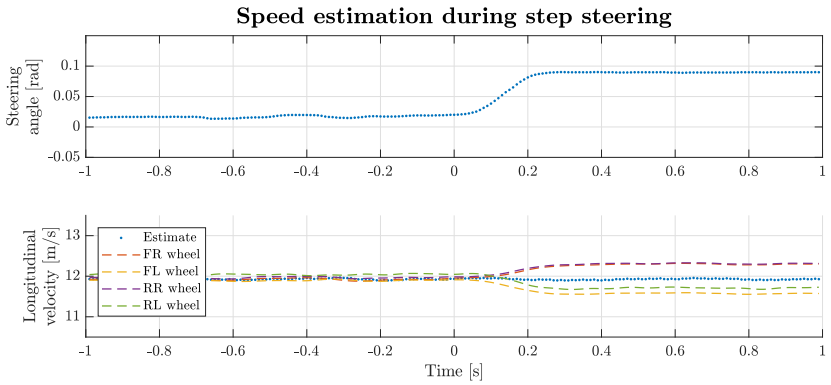

Figure 4.5: Speed estimation during step steering. There is a negligible effect during cornering on speed estimation during the transient of step steering which is important for the control.

4.4 Speed limiter

To achieve repeatability of maneuvers a speed limiter was designed. The goal of speed limiter is to limit to a speed defined by driver parametrization.

Following requirements needs to be met:

- Controller can only decrease the overall torque command to motors.
- Controller should be active only nearby desired speed limit.
- Settled value of speed should have a small deviation to the limiter setpoint.

The controller output is used as torque limitation and not as direct control of torque.

Vehicle has dominant longitudinal dynamics of the first order, and therefore a first order static transfer function can be assumed. This assumption is mostly correct but possible nonlinear situation - excessive wheel slippage might inadvertently activate the speed limiter. To solve this problem, a speed limiter should be used only with slip ratio controller activated. For speed limiter, a proportional controller is used. Steady state error is minimalized by a small proportional band but never entirely canceled. The algorithm used is a P controller with 0% output at a desired limited speed and with a proportional band of $1.5ms^{-1}$. It ensures that the speed will under every circumstance settle to $1.5ms^{-1}$ of desired.

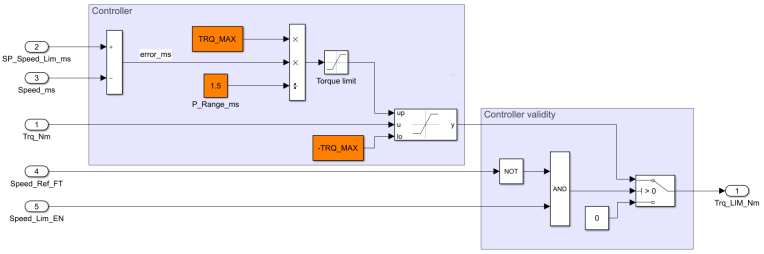

Figure 4.6: Speed limiter implementation. Software implementation of vehicle speed limiter in Simulink.

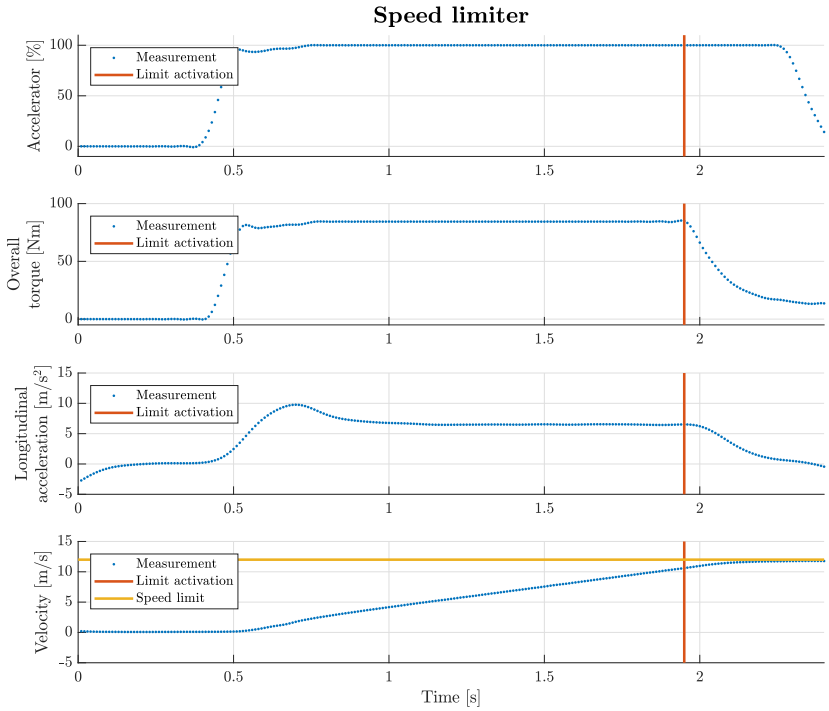

Figure 4.7: Speed limit step response. Example of speed limitation during test drive.

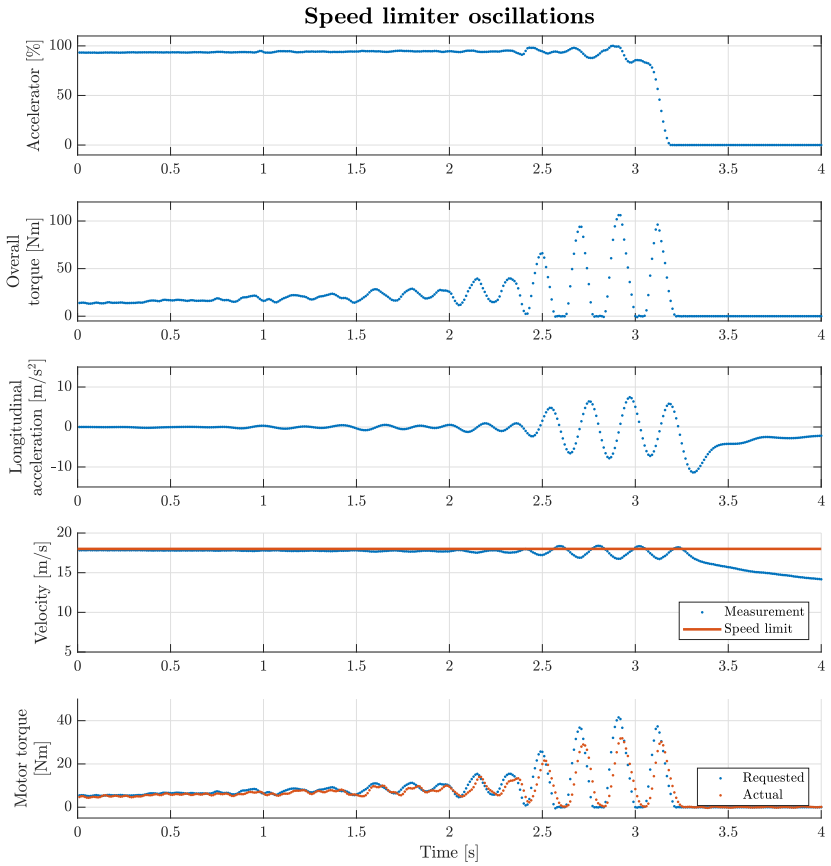

Figure 4.8: Speed limiter induced oscillations. Example of torque/speed oscillations due to motor controller slow response time and fast speed limiter feedback loop.

4.5 Slip ratio Controller

Maximum traction force (peak acceleration) is achieved at a certain slip level as explained in section 3.2. While producing maximum longitudinal acceleration (slip ratio) no additional lateral loading is possible, and vice versa. Therefore a working slip ratio controller is a good foundation for torque vectoring system that runs as a superior system.

Usually, the tire is loaded by combined forces and therefore combined slip should be used. For the sake of simplicity only longitudinal tire model is used for slip ratio controller. For longitudinal dynamics peak, tractive force slip ratio is around 10% for the used tire.

Following requirements need to be met:

- Controller can only decrease the torque command for individual motors.

- Controller should not have steady state error.

To satisfy these requirements a simple architecture of limiting PI controller with anti-windup using back-calculation method is used. The advantage of this control architecture is in its simplicity and ease of parametrization. For a control, only one wheel is considered. The tire model used is Pacejka Magic Formula as explained in section 3.2.1. Due to the tire model, a highly non-linear behavior is observed. For a vehicle, four quadrant control is considered. Formula SAE application has only need for forwarding direction quadrants therefore negative (regenerative) and positive (driving) torque is applied only while driving forward. The most important is positive torque slip ratio control for acceleration. Therefore it is implemented. Shown measurements on fig. 4.12 and fig. 4.11 are the best that were obtained the day of testing. Although there was a problem with anti-windup, the longitudinal performance was still increased.

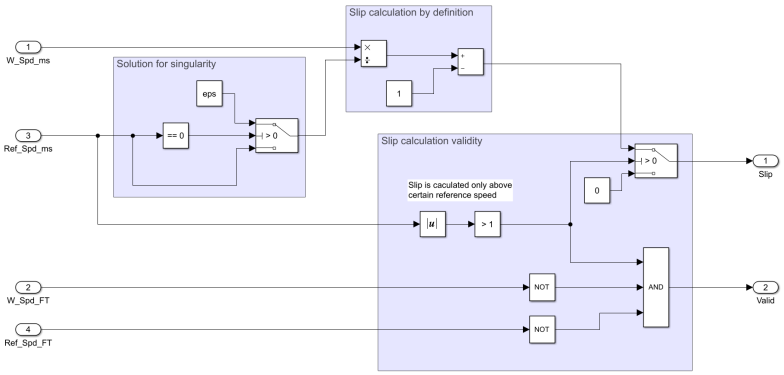

Figure 4.9: Slip ratio calculation. Slip ratio calculation implemented in Simulink.

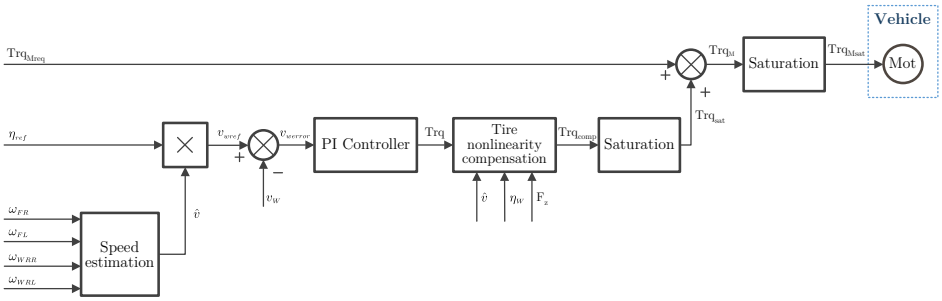

Figure 4.10: Control scheme of slip ratio control. The manipulation of torque for one motor is shown in this scheme.

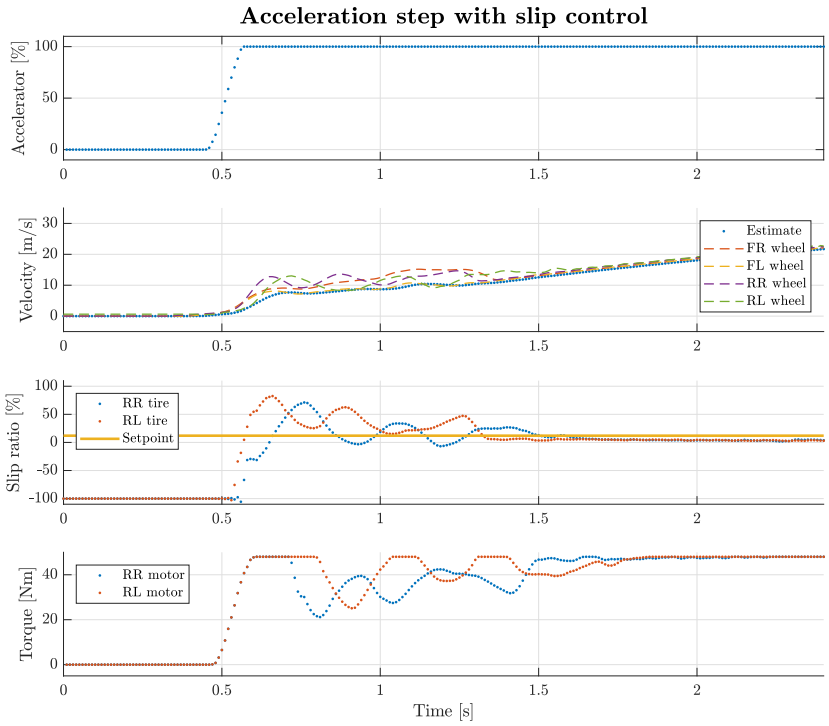

Figure 4.11: Acceleration step with slip ratio control. Example of acceleration with a limited slip by slip ratio controller. It can be seen that the slip ratio levels were contained.

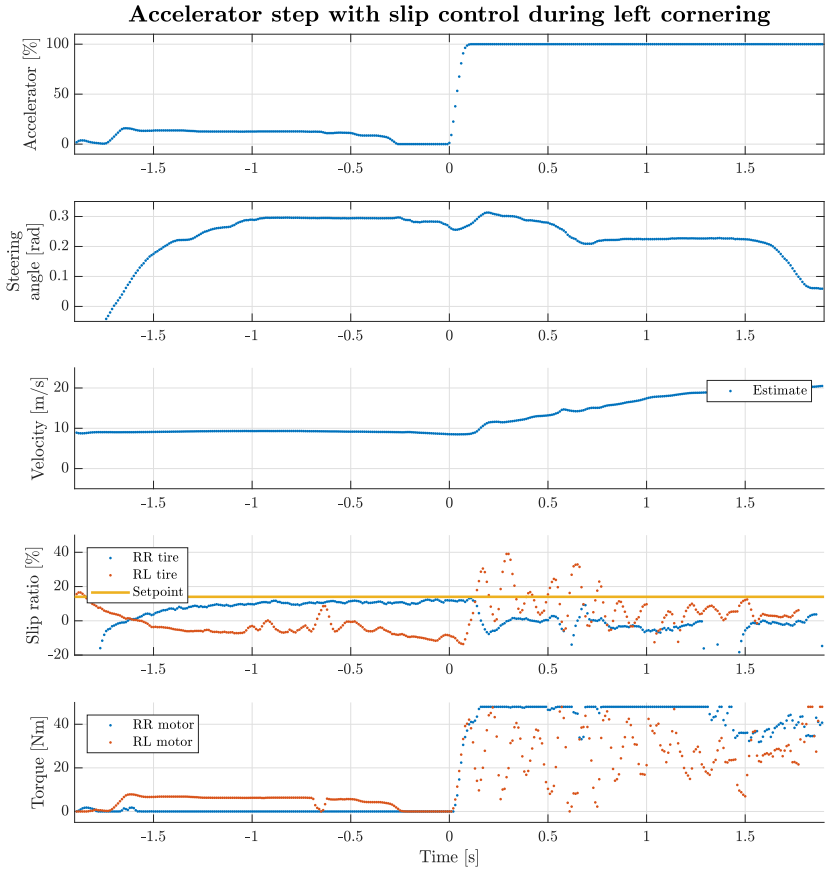

Figure 4.12: Acceleration step during cornering with slip ratio control. Example of slip limitation by slip ratio controller during cornering. It can be seen that slip ratio levels were contained, but due to weight transfer right wheels were in the linear region of slip characteristics while less loaded left wheels were on its peak of force characteristics.

4.5.1 Slip ratio controller compensation of tire non-linearity

The tire-road interaction is highly nonlinear as seen on fig. 4.13. There are other factors as driving resistance or combined slip, but these have smaller significance and therefore can be neglected for the sake of simplicity. Excessive wheel slip starts to develop when tire torque loading exceeds the capability of a tire. The slip ratio starts to build up rapidly because the resistance torque that is caused by traction force lowering with slip ratio above the peak force value. This behavior is of high importance for slip ratio controller design as the same controller output would result in different angular accelerations of a wheel for the different slip ratios of a tire. The compensation used increases the controller gain towards the peak force slip value as can be seen on fig. 4.13.

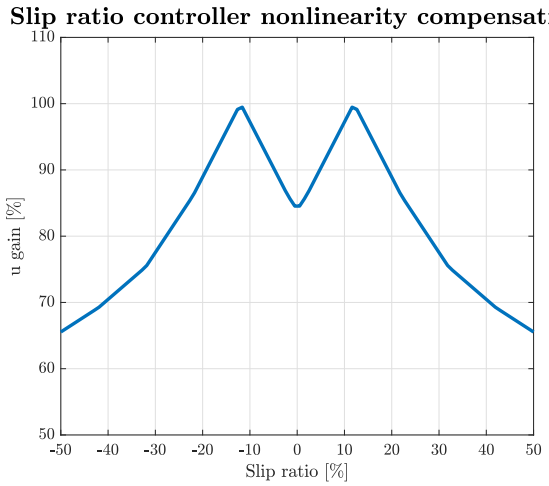

Figure 4.13: Tire non-linearity compensation. Slip ratio controller output amplified by a gain value dependent on actual slip ratio value.

4.6 Yaw rate reference generator

For a yaw rate tracking torque vectoring approach a yaw rate reference generator is used. Vehicle dynamics behavior defined by vehicle parameter is not meant to be overridden. A big influence on vehicle dynamics would add in the cost of energy consumption therefore vehicle needs to be carefully designed as a whole, and the TV controller helps to increase lateral acceleration while introducing disturbance rejection. With right torque distribution, the full potential of vehicle tires can be carried out. Furthermore, vehicle acts more neutral, and the effect of wear and heating on vehicle dynamics is suppressed.

These requirements had to be met for the generator:

- Simple to design, validate and adjust by a driver.
- Generator model matches the vehicle in most driving situations.
- Stable in all situations and yields a good result during the nonlinear regime.
- Generator model has increased response for low-speed driving.

The nonlinear single-track model explained in section 3.3.2 is used as it captures the dominant vehicle dynamics and is easily adjustable and understandable. Due to the single-track calculation stability problem at a lower speed, a kinematic model needs to be used. Kinematics model considered as a mass point with tire friction and aerodynamics forces is limited only for

low-speed use where dynamic effects are small. For higher speed, a constant speed single track model is used. The switching between models is based on speed and happens gradually using S-shaped blending. Models use steering angle, traction force, vehicle center of gravity speed to output yaw rate (see fig. 4.14). Single track model speed is controlled using a PI speed controller, and by feeding forward, the actual traction force commanded. Only forward driving is considered therefore the initial and minimal speed is defined for the single track model to achieve computational stability. This speed is considerably lower than the speed at which the models are switching.

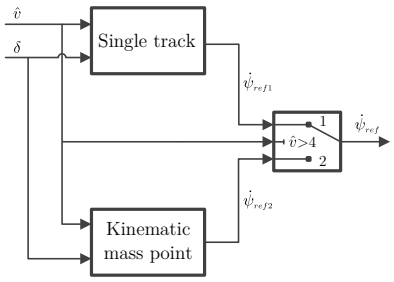

Figure 4.14: Yaw reference generator scheme. The two models are used and complementing each other for different vehicle speed.

4.7 Yaw damper

Lateral vehicle dynamics has similarities with airplanes pitch one dimensional dynamics. Lift coefficient curve is similar to the tire. A question arises if the control approach from aerospace could be transfered to land vehicles.

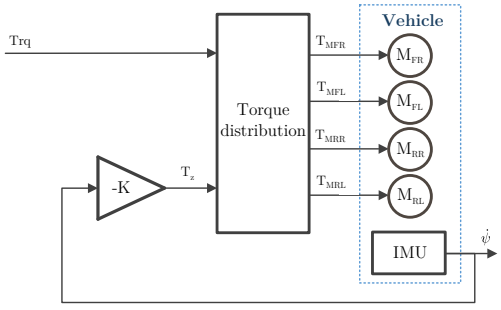

Figure 4.15: Control scheme of yaw damper. Yaw damper uses only yaw rate feedback.

4.8 Yaw rate controller

To modify the lateral vehicle dynamics a yaw torque is generated by redistribution of requested torque by driver between motors in the powertrain. Yaw torque value is calculated using the yaw rate controller [6, 9, 8]. The reference value of yaw rate and actual measured yaw rate from the inertial measuring unit is used as input. The PI controller is used with a back-calculation method for integral anti-windup. To correctly anti-windup, the actual applied yaw torque is calculated at the output of the distribution algorithm and fed bad to the controller. The yaw torque might be saturated due to motor torque characteristic limitations, derating of motors, driver settings. Correct handling of this saturation is important due to possible residual yaw torque calculated which would impact the drivability by a great amount.

On fig. 4.16 a yaw controller schematic can be seen. Simulink implementation is shown in fig. 4.17. The implementation of torque distribution algorithm is shown in fig. 4.18.

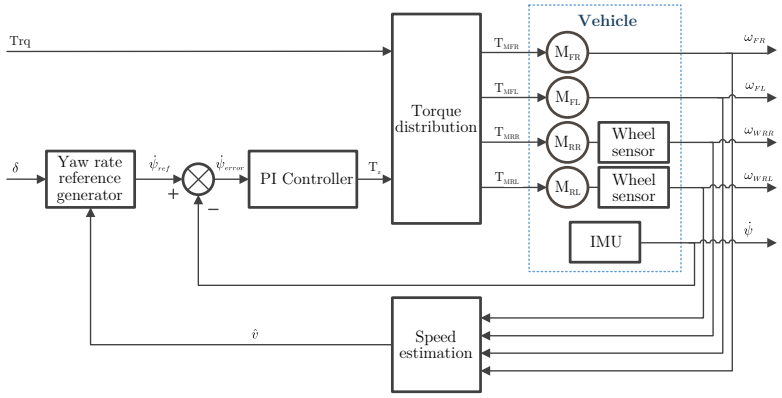

Figure 4.16: Control scheme of yaw rate tracking. Yaw rate controller uses yaw reference generator for yaw rate tracking.

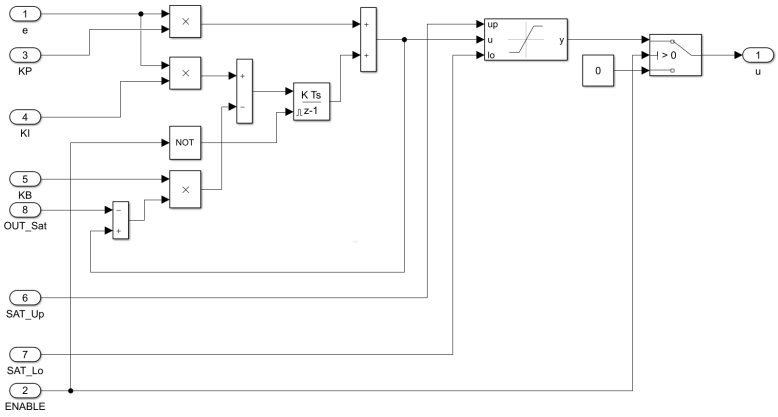

Figure 4.17: PI Controller implementation. Implementation of PI controller with back-calculation anti-windup.

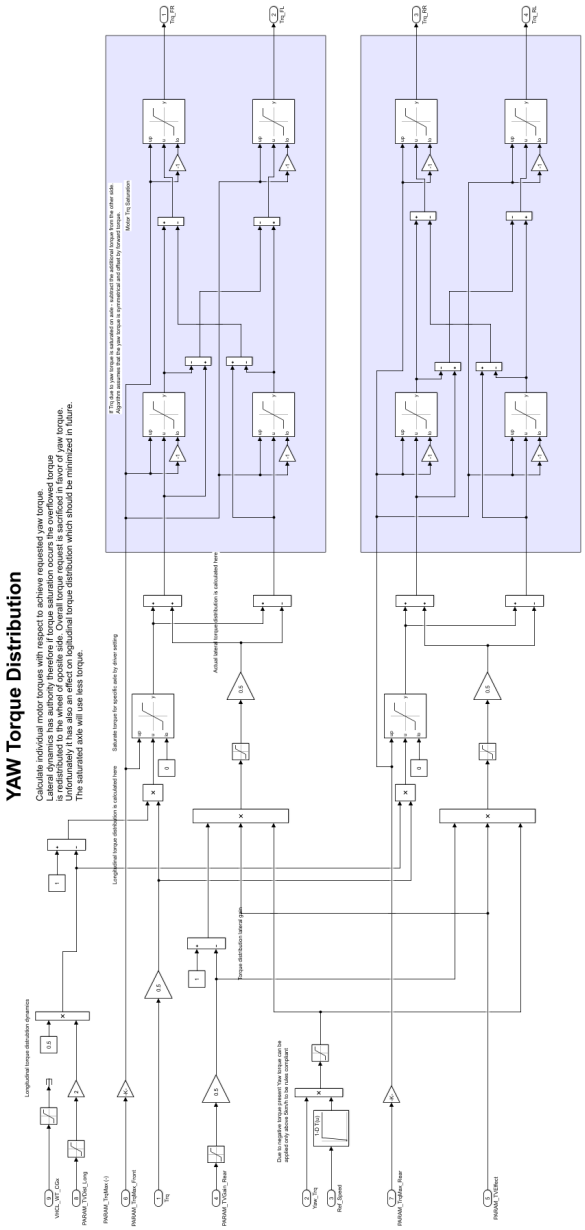

Figure 4.18: VDCU torque distribution. Implementation of torque distribution algorithm that fulfills the torque and yaw torque demands.

In the following pages, designed controllers are validated using IPG Carmaker multibody simulation model. Step steering output is in fig. 4.19, ramp steering results are shown in fig. 4.20. In fig. 4.21 a disturbance rejection is shown. The disturbance can be understood as sudden wind blow. Finally an understeering gradient is seen on fig. 4.22.

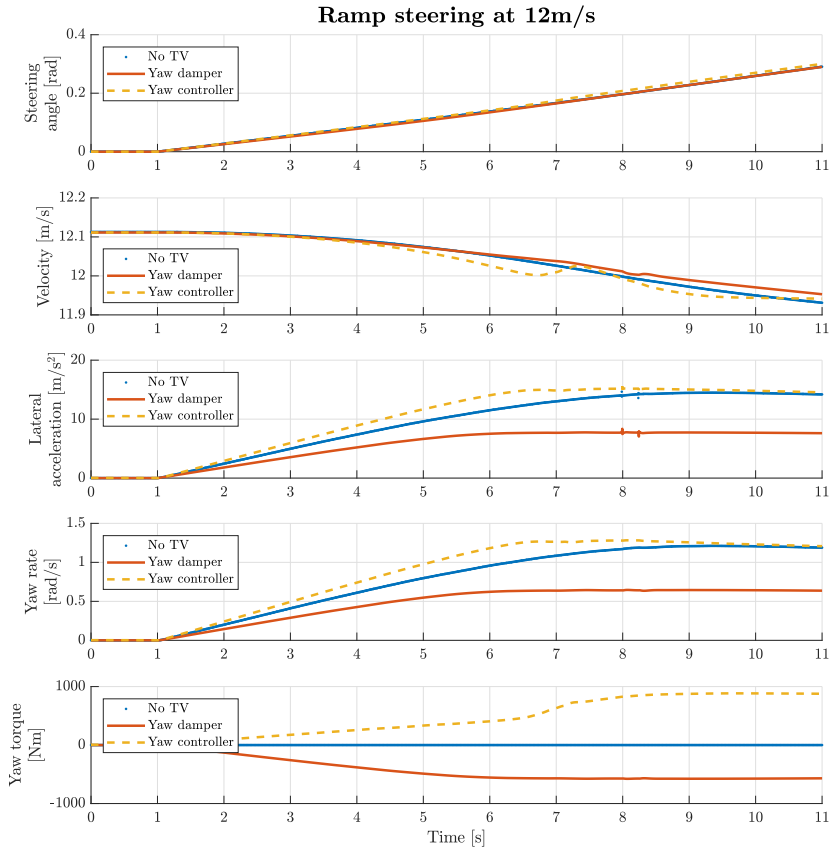

Figure 4.19: Validation of controller by ramp steering. Using the multi-body model it can be seen that the yaw rate response is more linear and increased for yaw controller. yaw damper decreases the yaw rate response as it does not distinguish between set point and disturbance.

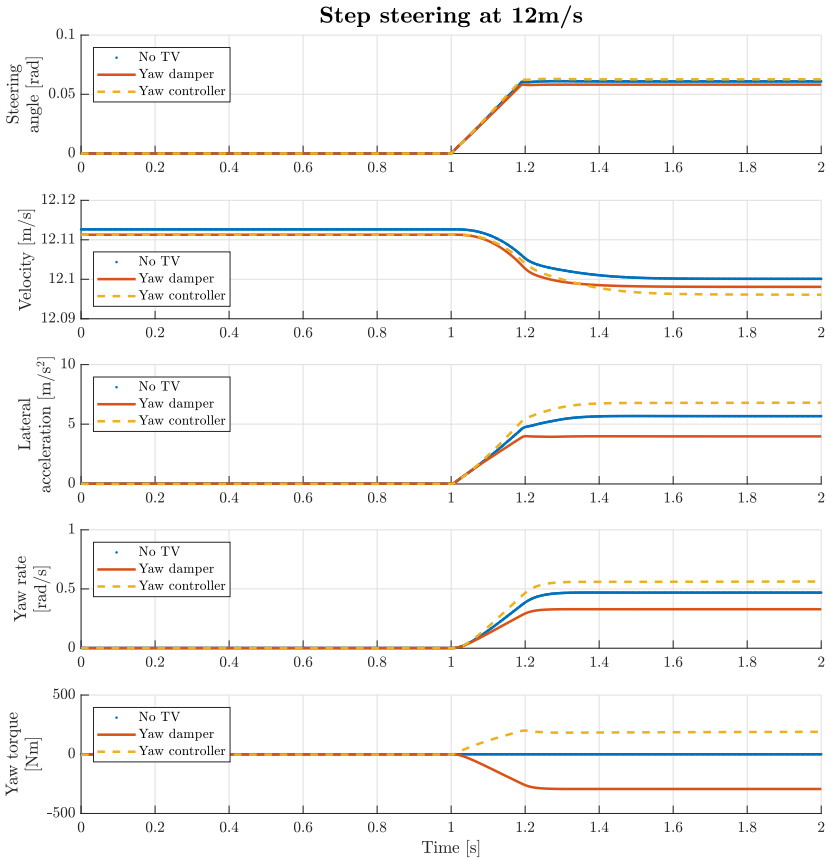

Figure 4.20: Validation of controller by step steering. The step steering yaw rate response is slightly improved using yaw controller but is decreased by yaw damper.

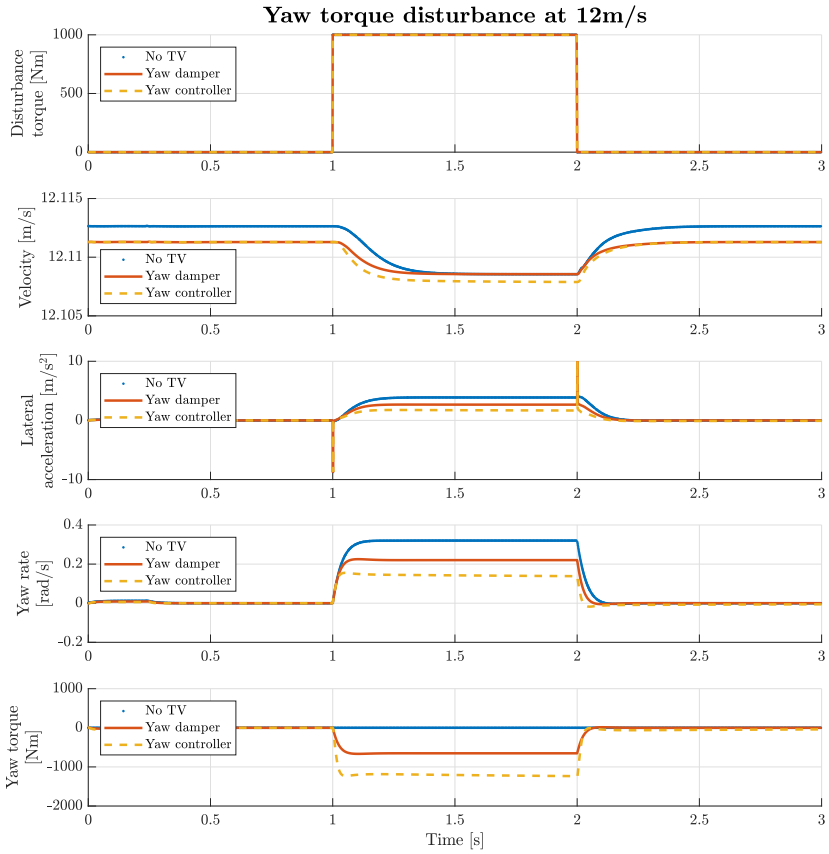

Figure 4.21: Disturbance rejection. External yaw torque was applied to the vehicle body in IPG Carmaker. The controllers have similar behavior in this case but the absolute values are better for yaw controller.

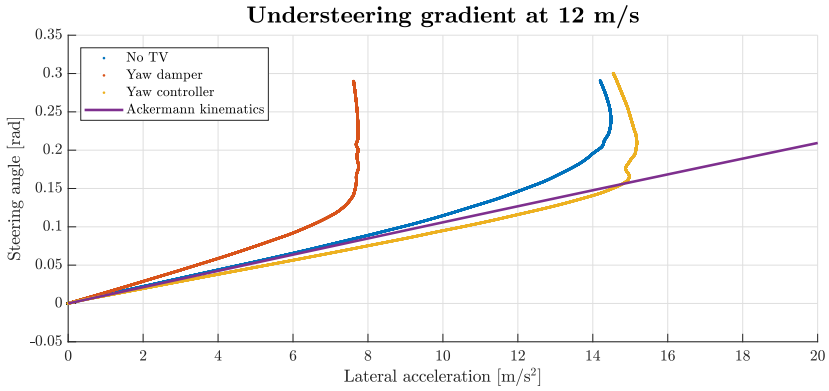

Figure 4.22: Simulated understeering gradient. Simulated understeering gradient on IPG Carmaker multibody model gives a good illustration of the different controllers steady state cornering characteristics. Plain yaw damper decreases vehicle cornering performance while yaw controller increases vehicle cornering performance.

Chapter 5

Experimental results and testing

5.1 Virtual test driving

Due to budget and time constraints for vehicle drive testing, it is useful to find other means of testing - virtual test driving. Predefined maneuvers are used as part of the objective testing which is not enough to get the whole picture of vehicle dynamics. A vehicle is driven by a human and therefore driver-in-the-loop (DIL)[1] testing approach complements (see fig. 5.1). Evaluation is then possible during the whole design process from vehicle model to controller development and parameters tuning. By driving the same maneuvers and same track, the driver gets an appropriate feeling for actual changes. There is also a benefit from understanding the effect of parameters tuning. Required time for vehicle drive tests is therefore further reduced.

Visualization and force feedback helps to expand the understanding as graphical output is insufficient for getting the whole picture about vehicle dynamics. Steering wheel force feedback is also affected by the introduction of the vehicle dynamics controller.

The solution presented uses a simulation platform consisting of Thrustmaster T300 RS steering wheel with pedals mounted on racing seat and connected to PC (see fig. 5.2). A large curved LCD screen is used to achieve an appropriate view angle. It is advantageous that the IPG Carmaker[2] simulation software can be used in the whole design process to virtual test driving just by installing a cockpit package add-on. Simulink[3] running the vehicle controller implementation is interfacing the IPG Carmaker.

Unfortunately sound is not supported without using third-party software. The sound is an important feedback factor in virtual driving due to the absence of some of the feedback factors as forces acting upon one's body.

[1] IPG AUTOMOTIVE GmbH. `www.ipg.com`
[2] IPG AUTOMOTIVE GmbH. `www.ipg.com`
[3] The MathWorks, Inc. `www.mathworks.com`

Virtual testing in the used form can assist the development, but real driving tests need to be still carried out.

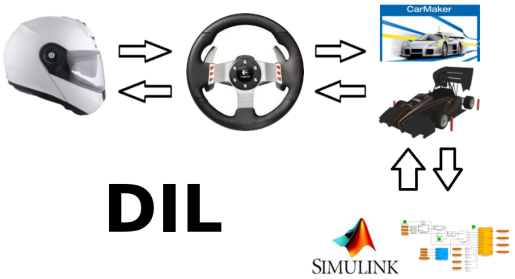

Figure 5.1: DIL structure. DIL structure used in virtual test driving.

Figure 5.2: Virtual test driving. Testing the designed controller by virtual test driving on simulation platform that connects Simulink with IPG Carmaker and steering wheel.

5.2 Restbus simulation

Due to the dangerous nature of a race vehicle a change into the ECU that manipulates motor torque needs to be thoroughly investigated before the actual integration. It is necessary that the unit reliably interacts with the rest of the vehicle ECUs through CAN bus and that there is no faulty behavior. This can be tested by the implementation of a simple panel in CANoe[4] environment from Vector. A CAN network database file (DBC)[5] is required to describe the vehicle CAN bus network. Developed graphical interface on fig. 5.3 shows the components as an accelerator pedal, steering wheel, switches .etc to test the correct functions of the system. Testing with this panel is manual, and specific steps need to be followed with good knowledge

[4] Vector Informatik GmbH. `https://www.vector.com/`

[5] Vector Informatik GmbH. CANdb++ `https://www.vector.com/int/en/products/products-a-z/software/candb-adminj1939/`

of the designed system. Required time for with the real vehicle is reduced, and safety is increased.

Figure 5.3: VDCU Restbus simulation graphical panel. Testing the VDCU by use of restbus simulation just before integration into vehicle.

5.3 Experimental results

Due to the time constraints the tests were performed in December under unpleasant conditions with heavy wind, temperature few degrees above freezing point and only with two hours of useful daylight. Previous tests were scrubbed as a result of technical problems with the vehicle. One such unfortunate problem rendered the vehicle unusable for one month.
Test maneuvers were developed and evaluated beforehand using IPG Carmaker simulation as shown with controller development in chapter 4. Similar maneuvers were performed for model validation in section 3.4. The parametrization of controllers was performed by driver during the drive using graphical user interface (GUI). Changes are convenient to make by incremental buttons and absolute potentiometers. Small adjustments are possible while driving and big while standstill. Data were logged by Vector GL 1010 CAN Bus logger[6].

[6]Vector Informatik GmbH. `https://www.vector.com/`

Figure 5.4: Vector GL1010 CAN bus logger. Used for datalogging by capturing CAN bus communication.

All essential events and logical steps were written using custom made testing sheet and in time as they happened. This information were usefull for later analysis. Data were recorded asynchronously and so in the way they are received. After a few tests drive the data were downloaded and analyzed using CANoe graphical analyses tool looking for the needed measurements and possible problems. After the test day, data of interests were converted to a mat file. Using MATLAB, the data were resampled for uniform timestamps and the analyses, and further calculations can be performed. The measurements were also fed back to the control system in offline open-loop simulation to expand the understanding of controller behavior further.

A yaw rate tracking controller was finally implemented into the vehicle and tested. Presented data are the results of the successful TV implementation. There is a big portion of drive feels the graphs hardly describe. Steering wheel feedback was noticeably modified why lateral stability greatly increased. Due to the implementation of the slip ratio controller, the longitudinal behavior was also noticeably better. Resultant vehicle handling makes performance driving on the limit easier with less unpredictable factors.

Following fig. 5.6 compares the lateral vehicle response to ramp steering input with and without TV. The steering ramp was chosen with the smallest possible slope by space restrictions of the place where the tests were performed. This tests should show the vehicle steady-state cornering, and therefore an understeering gradient can be then plotted on fig. 5.7. Increased yaw rate and more linear response following the input with some nonzero control error can be seen..

[6]Vector Informatik GmbH. `https://www.vector.com/`

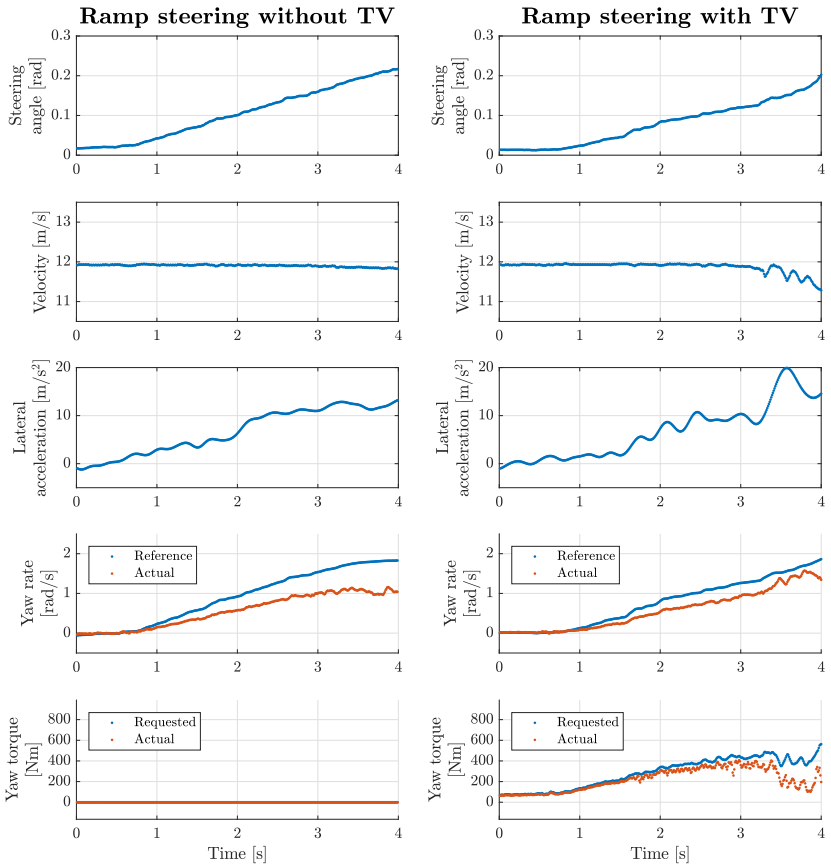

Figure 5.5: Validation of TV implementation using ramp steering. An increase of yaw rate can be observed using the torque vectoring.

Measured transient dynamics are shown on fig. 5.5. There is a negligible change to transient response. The yaw rate absolute value was increased with TV implemented.

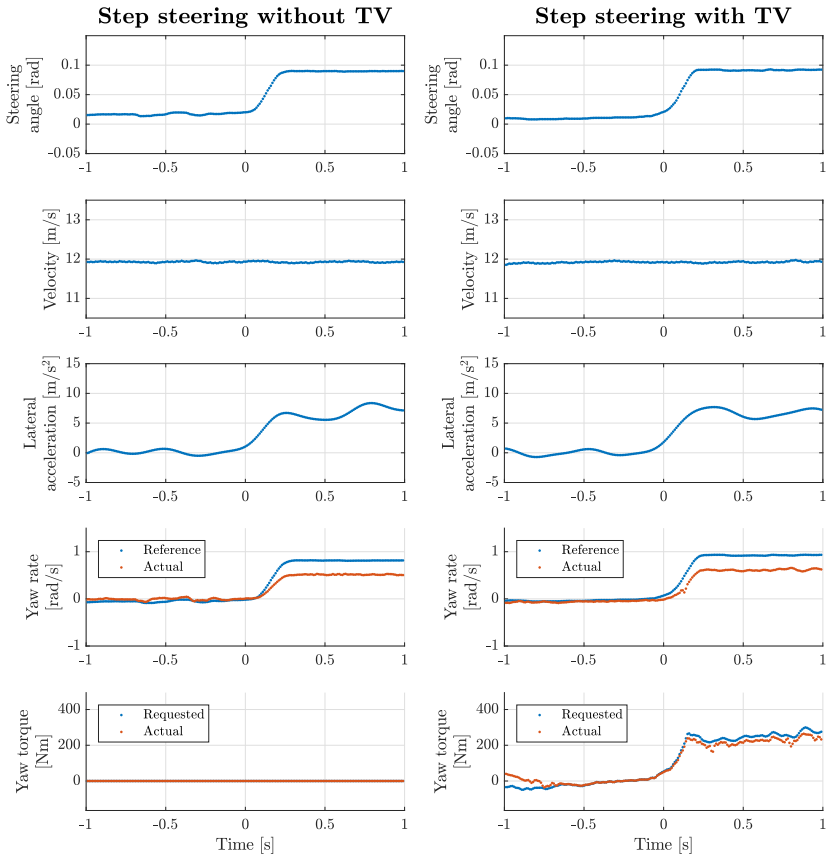

Figure 5.6: Validation of TV implementation using step steering. The step steering response is slightly improved using torque vectoring.

Following understeering gradient fig. 5.7 was obtained by the plot of steering angle to lateral acceleration using ramp steering data. During all situation, the vehicle understeered as shown in fig. 1.1. It can be seen that the response is more linear at a lower speed while only a small lateral acceleration is achieved. With higher speed, the similarity to the kinematic model is being lost. This is due to achieving peak forces and slips on tires resulting in non-linear behavior. TV system significantly improves the vehicle in all speeds.

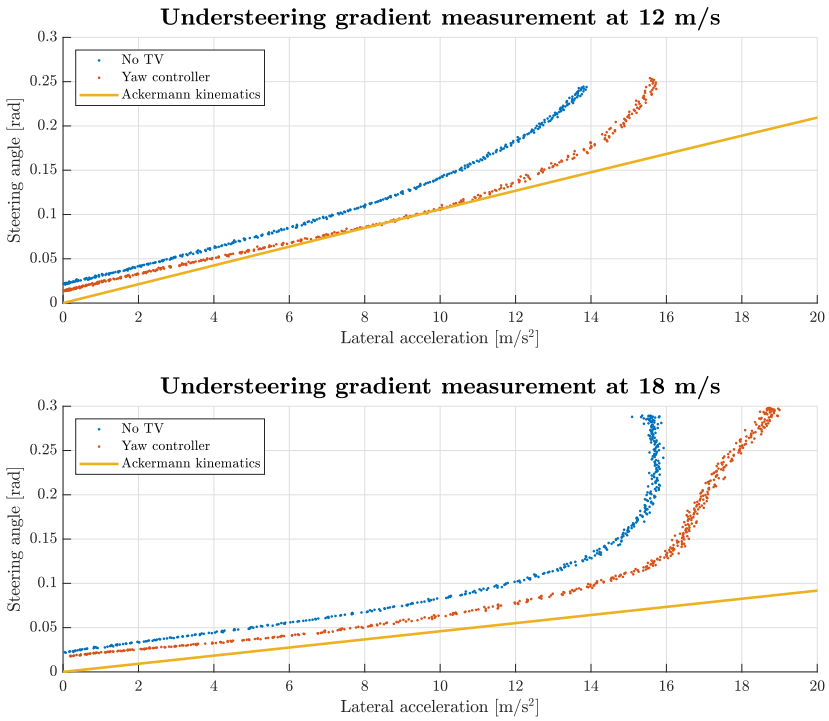

Figure 5.7: Measured understeering gradient. Understeering gradient is varied by torque vectoring implementation. Lateral acceleration response on ramp steering is more linear, faster and lateral acceleration saturates at higher value.

On the fig. 5.8 a long term effect of torque vectoring can be seen. By using the TV system, some motors might be loaded more than others due to track specifics. This particular histogram was obtained from a race in Estonia with only an open-loop controller that was used it that time.

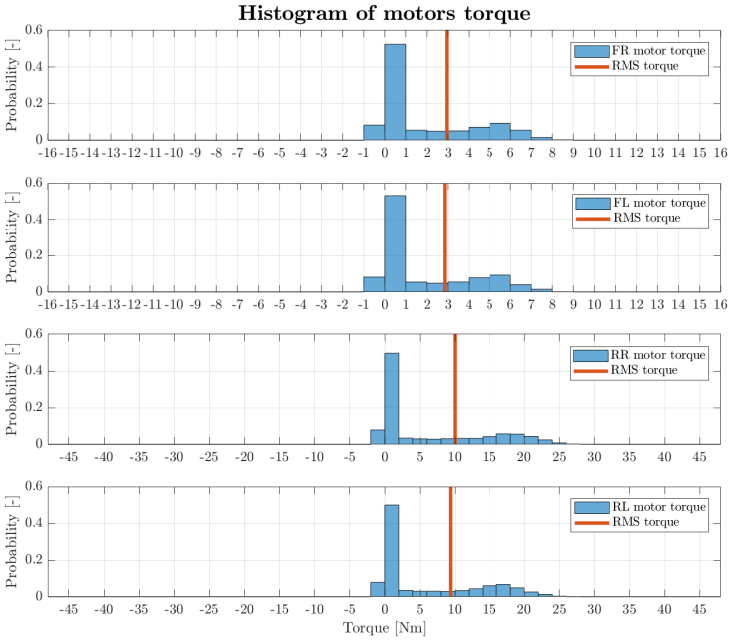

Figure 5.8: Motor torque histogram during race. By use of torque vectoring a difference between left and right motors torque demands during the race length are existing. In this case motors on right side were loaded more.

Chapter 6

Conclusions

In chapter 3 vehicle models were presented. A single track model implementing aerodynamic lift force was shown in section 3.3.2 while parametrization of high fidelity multibody model was detailed in section 3.3.3. Different tire models of CPI and STI were explained, and Pacejka Magic Formula was used within the single-track model. All models were validated by measured data from previous experimental drive tests.

Chapter 4 presents the design and implementation of vehicle dynamics controller. Yaw damper was designed in section 4.7 while yaw rate tracking controller is presented in section 4.8 with used yaw rate reference generator described in section 4.6. In section 4.5 a slip ratio controller design is detailed.

Experimental results are shown in chapter 5. Due to previous mechanical issues, the tests were greatly reduced and the data acquired were compromised. By understeering gradient comparison, It can be seen on fig. 5.7 that the introduction of torque vectoring improved the lateral vehicle dynamics performance. Finally, virtual test drives are presented in section 5.1 and restbus simulation was described in section 5.2.

Chapter 7

Future work

The goals were fulfilled, and the torque vectoring solution was successfully implemented and tested in 4WD formula student electric vehicle. Tests were successful, but further improvements are proposed in this chapter to increase the performance even further. The vehicle was built by a group of students in a limited time of one year. Therefore the systems have different quality levels and would be improved in future vehicle models.

- **Better model fit** - there is a room for improvement regarding the vehicle models. By developing single track model further, its implementation in yaw rate reference generator would yield more accurate results under broader conditions. Multibody model improvements would positively affect the design process and testing of controllers. Required time using the vehicle for experimental drive tests would be further decreased.
- **Slip ratio controller implementation in motor controller** - within the thesis a speed control feedback loop was integrated into VDCU. Feedback control loop quality is negatively affected by CAN communication due to significant time constraints of the system. A solution to use the speed control loop implemented inside the motor controller is proposed. The inputs to the motor controller are a speed setpoint value and output torque saturation value. Torque output saturation is a function of the driver accelerator pedal. During no-slip operation only torque saturation is varied as speed setpoint would be left at maximum. Therefore the speed controller would be saturated and not affecting the torque command. During excessive slippage, the speed setpoint is decreased, and the speed control loop in the motor controller would start controlling the motor speed. The communication delay uncertainty affecting the feedback loop is eliminated. This makes the control more precise while also increasing its frequency [20].
- **Making the solution rules compliant** - as noted in chapter [1] current

implementation of the torque vectoring does not comply with FSAE rules due to the vehicle design limitations. The solution used generates yaw torque independently of the torque requested by the driver. Implemented torque vectoring does not adhere to the rule that no positive torque should be applied to motors while driver torque request is zero [1]. Design changes in vehicle regenerative braking and torque vectoring system are needed.

- **Estimation of additional states** - a few states are currently estimated. By integration of INS, a slip angle estimate could be introduced. Using INS, the estimates quality of vehicle speed and load could be further increased. Longitudinal reference speed at each wheel carrier should be estimated to improve the slip ratio controller further.

- **Better measurements quality** - measurements of wheel speed and inertial sensors are unreliable. Wheel speed incremental sensor has an unreliable output signal which was not correctly processed within the ECU. This lead to slip ratio control quality issues. Acceleration data measured by IMU needed heavy filtering due to small attenuation of vibration mechanically and software. Inertial data can be improved by further development of IMU or by using off-the-shelf INS. Due to the nature of this project It is sometimes challenging to get everything ready at sufficient quality. Responsibility could not always be taken for the problems.

- **Faster response time of actuators** - motor controller significantly filters the desired torque value input. Therefore a response time is increased, and phase delay added which destabilizes the system when higher feedback control gains are used. This could be observed in the example of a speed limiter on fig 4.8.

- **Dynamic longitudinal torque distribution** - dynamic longitudinal distribution should be used to further utilize the available tire grip. Currently, for the sake of simplicity a user parametrized longitudinal distribution was used. It was only modified by operation of slip ratio controller. Suggested solution should use estimated tire load and manipulation of reference slip ratio limit for each wheel individually. Implementing a feedforward would further increase the quality as slip ratio controller would not be less used.

- **Online telemetry parametrization** - To further reduce needed testing time online telemetry could be used. Implementing a CAN Calibration Protocol (CCP) it would be possible to change parameters in ECU during the actual run.

Bibliography

[1] Formula SAE rules 2017/2018. https://www.fsaeonline.com/content/2017-18%20FSAE%20Rules%209.2.16a.pdf. Accessed: 2019-08-01.

[2] IPG AUTOMOTIVE GmbH. www.ipg.com. Accessed: 2019-08-01.

[3] J. D. Anderson. *Introduction to Flight*. McGraw-Hill, New York, 5th edition, 2004.

[4] A. Bergmann. Benefits and drawbacks of model-based design. *KMUTNB International Journal of Applied Science and Technology*, 7:15–19, 09 2014.

[5] eForce FEE Prague Formula. Czech Technical University in Prague. https://eforce.cvut.cz/. Accessed: 2019-08-01.

[6] J. Ghosh, A. Tonoli, and N. Amati. A torque vectoring strategy for improving the performance of a rear wheel drive electric vehicle. In *2015 IEEE Vehicle Power and Propulsion Conference (VPPC)*, pages 1–6, Oct 2015.

[7] T. D. Gillespie. *Fundamentals of vehicle dynamics*. SAE Internation, Berlin, 1st edition, 1992.

[8] G. Kaiser, F. Holzmann, B. Chretien, M. Korte, and H. Werner. Torque vectoring with a feedback and feed forward controller - applied to a through the road hybrid electric vehicle. In *2011 IEEE Intelligent Vehicles Symposium (IV)*, pages 448–453, June 2011.

[9] G. Kaiser, Q. Liu, C. Hoffmann, M. Korte, and H. Werner. Torque vectoring for an electric vehicle using an lpv drive controller and a torque and slip limiter. In *2012 IEEE 51st IEEE Conference on Decision and Control (CDC)*, pages 5016–5021, Dec 2012.

[10] J. Kong, M. Pfeiffer, G. Schildbach, and F. Borrelli. Kinematic and dynamic vehicle models for autonomous driving control design. In *2015 IEEE Intelligent Vehicles Symposium (IV)*, pages 1094–1099, June 2015.

[11] H. Marzbani, D. Vo, A. Khazaei, M. Fard, and R. Jazar. Transient and steady-state rotation center of vehicle dynamics. *Procedia Computer Science*, 112:1404–1411, 12 2017.

[12] R. C. Nelson. *Flight Stability and Automatic Control*. McGraw-Hill Education, New York, 2nd edition, 1997.

[13] H. B. Pacejka. *Tyre and vehicle dynamics*. Butterworth-Heinemann, Oxford, 1st edition, 2002.

[14] H. B. Pacejka. *Tyre and vehicle dynamics*. Butterworth-Heinemann, Oxford, 2nd edition, 2006.

[15] J. P. Pauwelussen. *Essentials of Vehicle Dynamics*. Butterworth-Heinemann, HAN University of Applied Sciences, 1st edition, 2013.

[16] R. Rajamani. *Vehicle Dynamics and Control*. Rajesh Rajamani, 2006.

[17] G. Rill. Tmeasy – a handling tire model based on a three-dimensional slip approach. 01 2013.

[18] SAE J 670:2008(E). Vehicle Dynamics Terminology. Standard, Society of Automotive Engineers, Warrendale, US, Jan. 2008.

[19] V. Scheuch, G. Kaiser, M. Korte, P. Grabs, F. Kreft, and F. Holzmann. A safe torque vectoring function for an electric vehicle. In *2013 World Electric Vehicle Symposium and Exhibition (EVS27)*, pages 1–10, Nov 2013.

[20] J. Ulrich. Torque Vectoring – KIT Team Sharing Vehicle Controls Success Story. `https://blogs.mathworks.com/racing-lounge/2017/11/22/torque-vectoring-ka-race-ing/`. Accessed: 2019-08-01.

[21] U. H.-J. Unrau and Z. J. TYDEX-Format. Standard, Universität Karlsruhe (TH), Karlsruhe, Sept. 1997.

[22] A. v. Zanten. *Regulace jízdní dynamiky: jízdní bezpečnost motorových vozidel*. Robert Bosch, Praha, 1. české vyd. edition, 2001.

Appendix A

Control software Simulink schematics

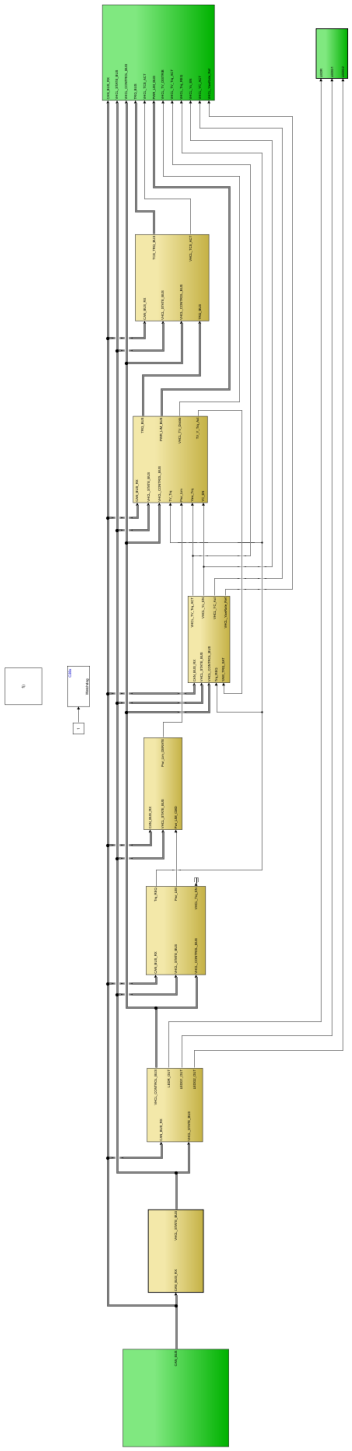

Figure A.1: VDCU code overview. Upper program level view where all software sub components can be seen connected. CAN inputs are on left and CAN outputs are on right side.

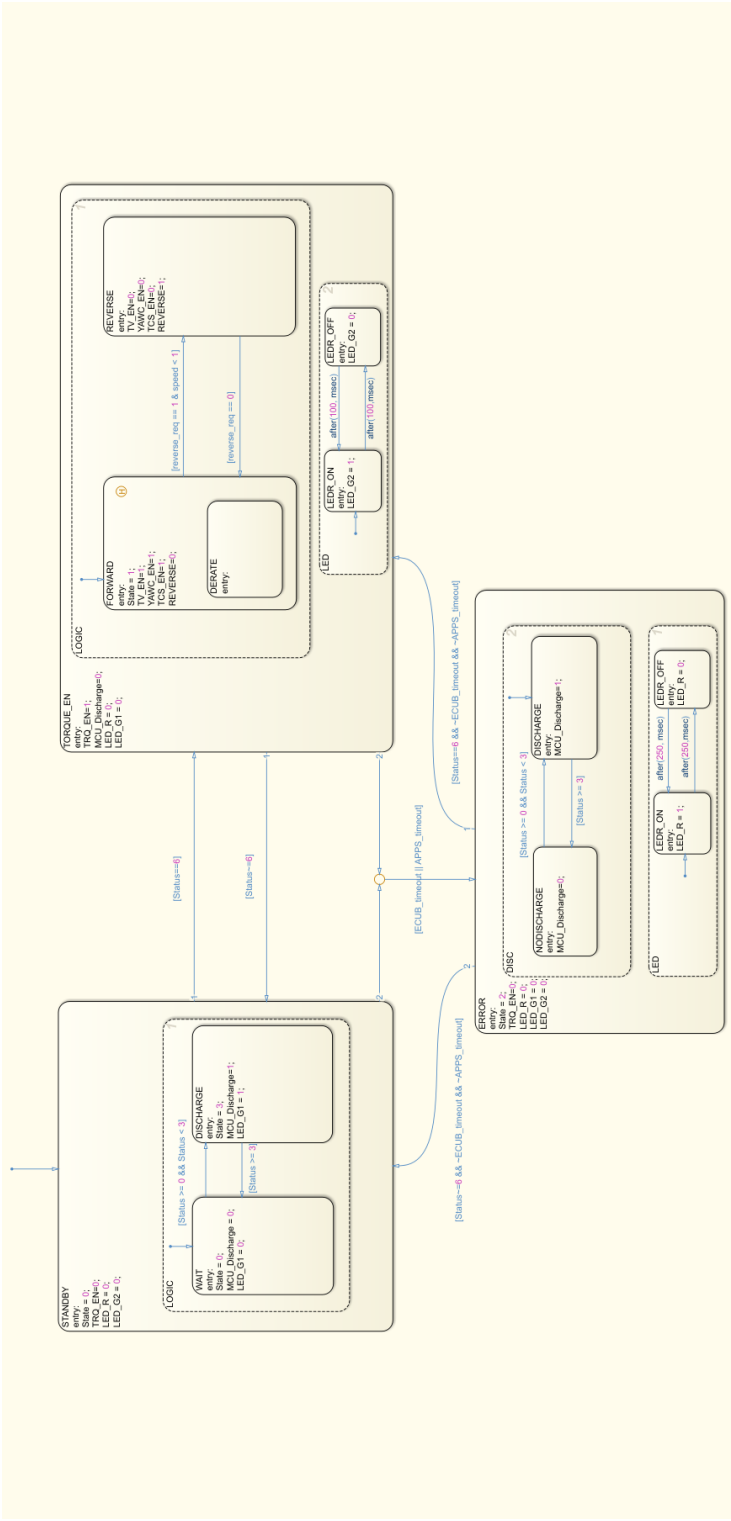

Figure A.2: State machine. For logical control of vehicle a state machine was designed using Simulink Stateflow diagram.

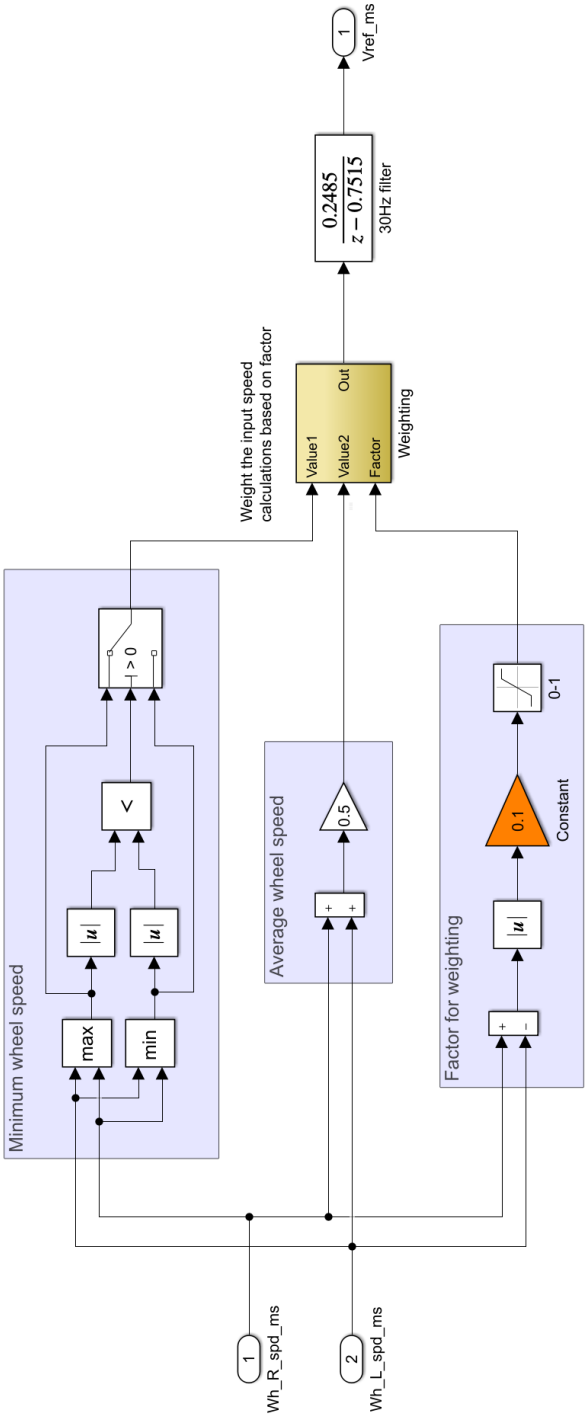

Figure A.3: Speed estimator implementation. Software implementation of vehicle reference speed estimator in Simulink by weighting between minimum and average of wheel speeds.

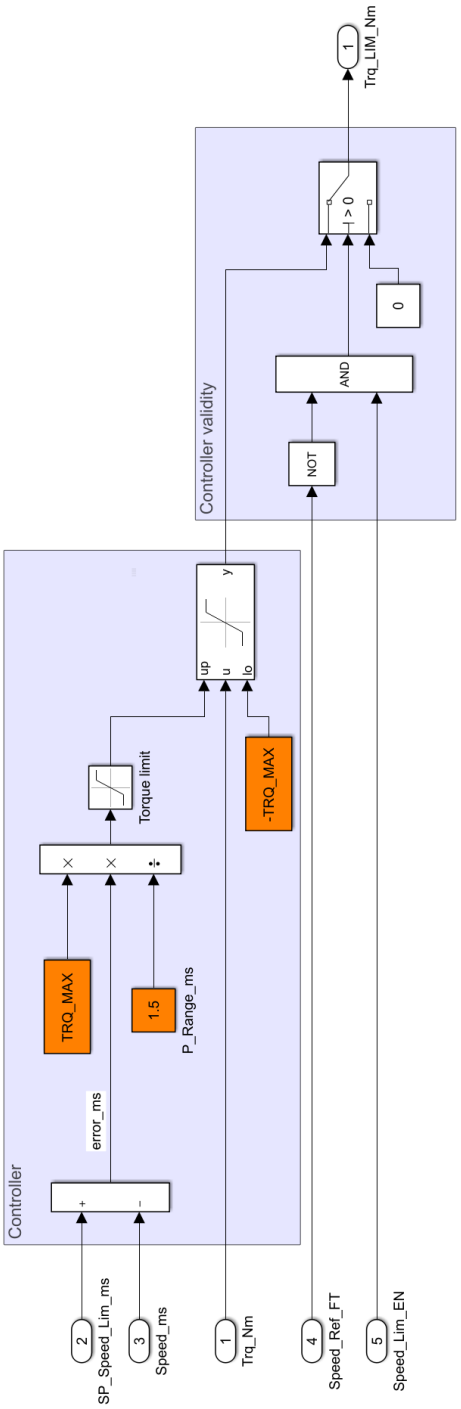

Figure A.4: Speed limiter implementation. Software implementation of vehicle speed limiter in Simulink.

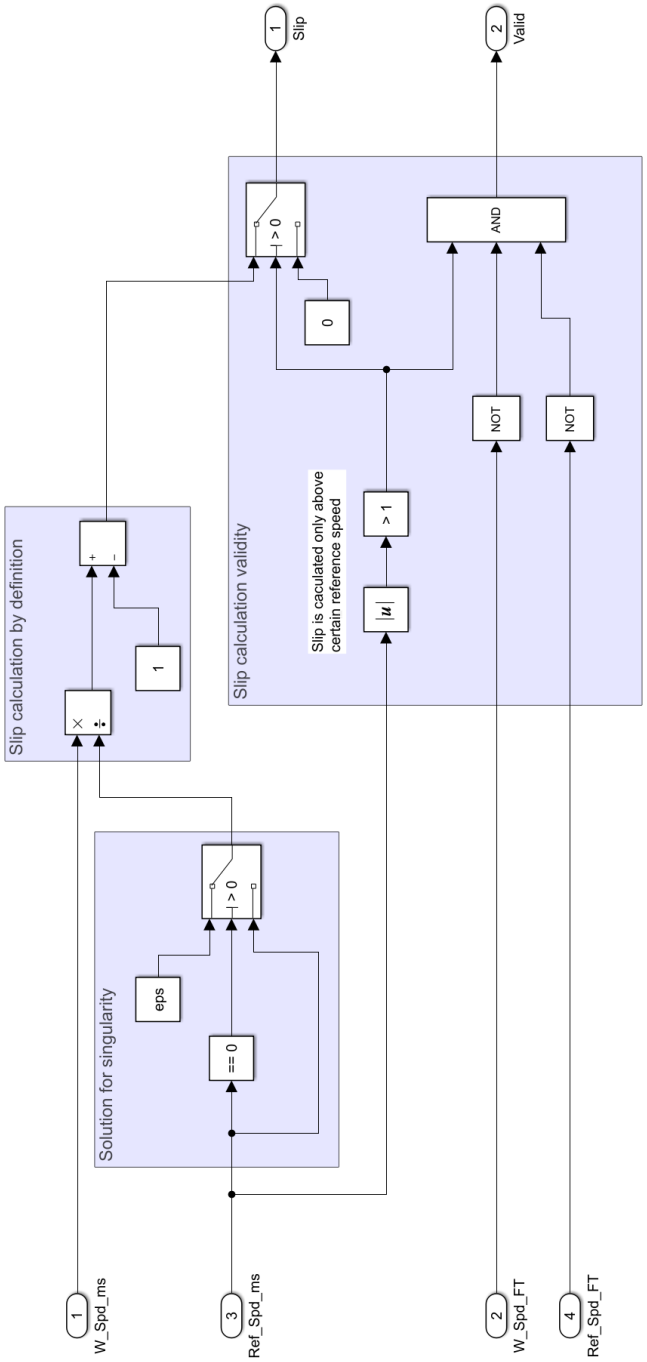

Figure A.5: Slip ratio calculation. Slip ratio calculation implemented in Simulink.

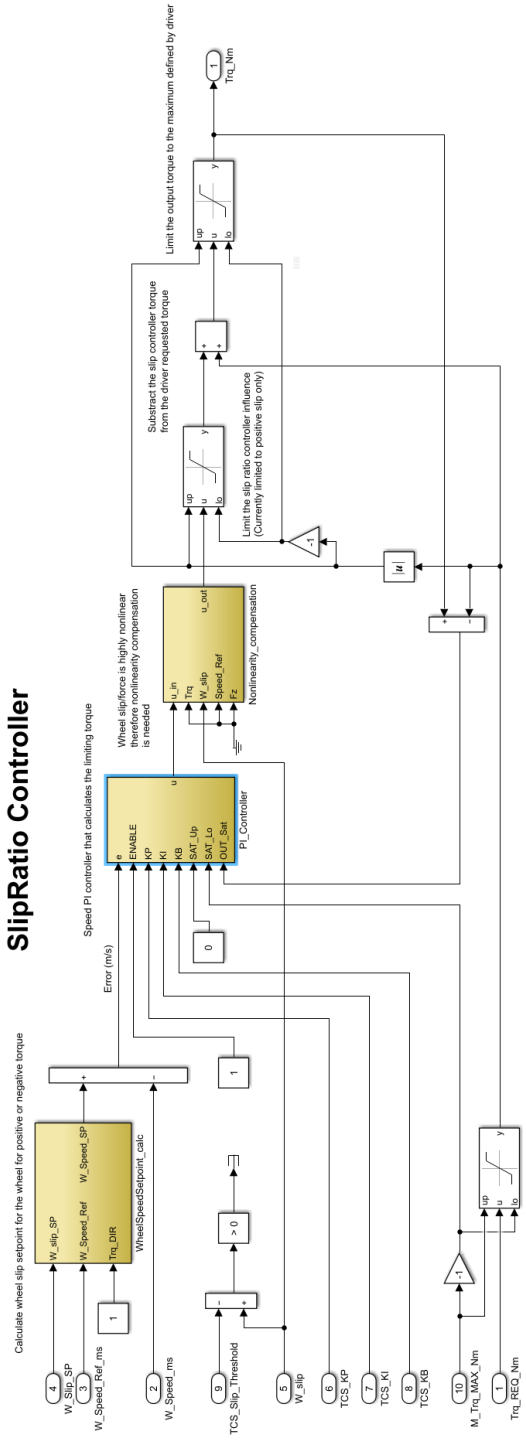

Figure A.6: Slip ratio controller. Software implementation of slip ratio controller in Simulink. The one controller manipulates all 4 wheels as it uses vectors for calculation. Anti-windup was designed to cover various saturation of controller output by motor operating limits and driver vehicle setup adjustments.

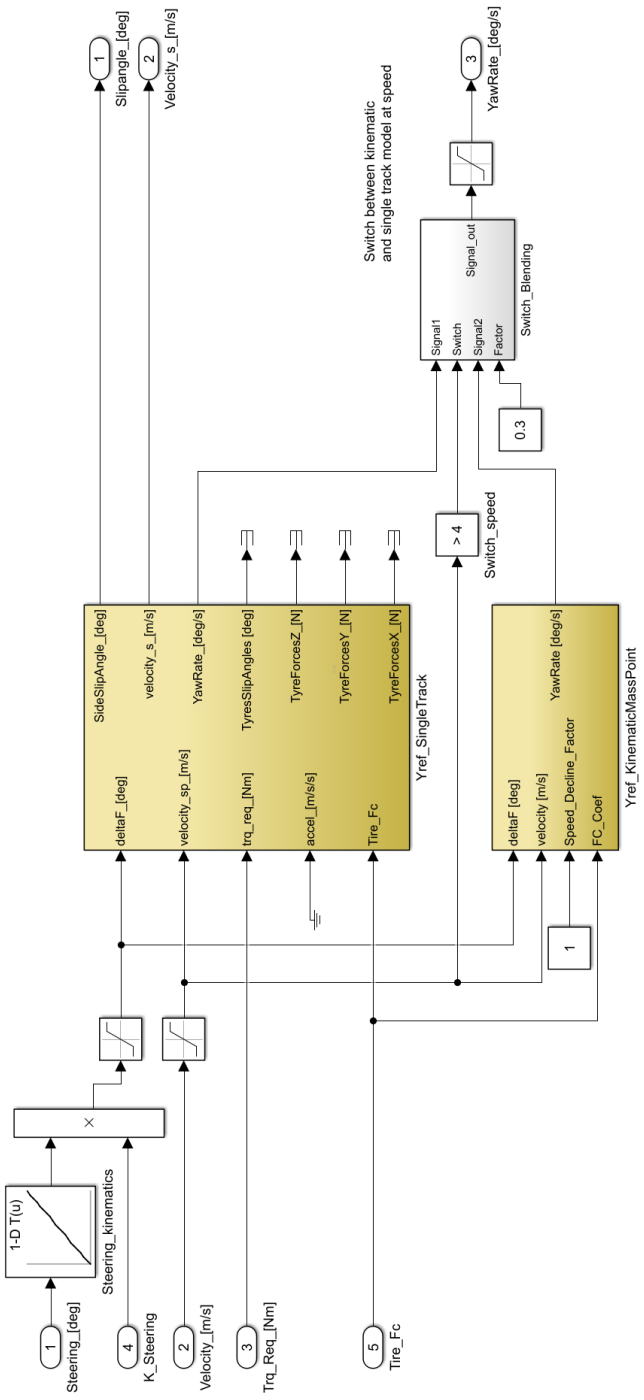

Figure A.7: VDCU yaw rate reference. Implementation of yaw rate reference model in software.

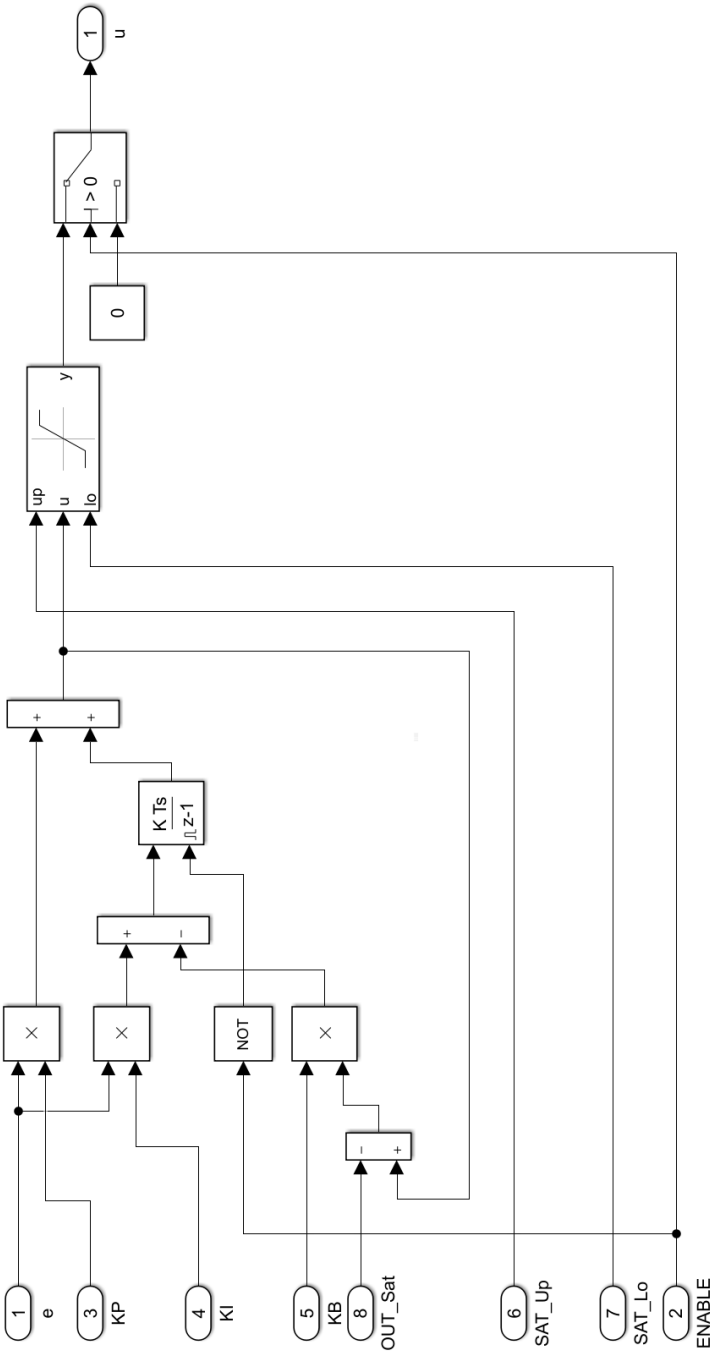

Figure A.8: PI Controller implementation. Implementation of discrete PI controller with backcalculation antiwindup.

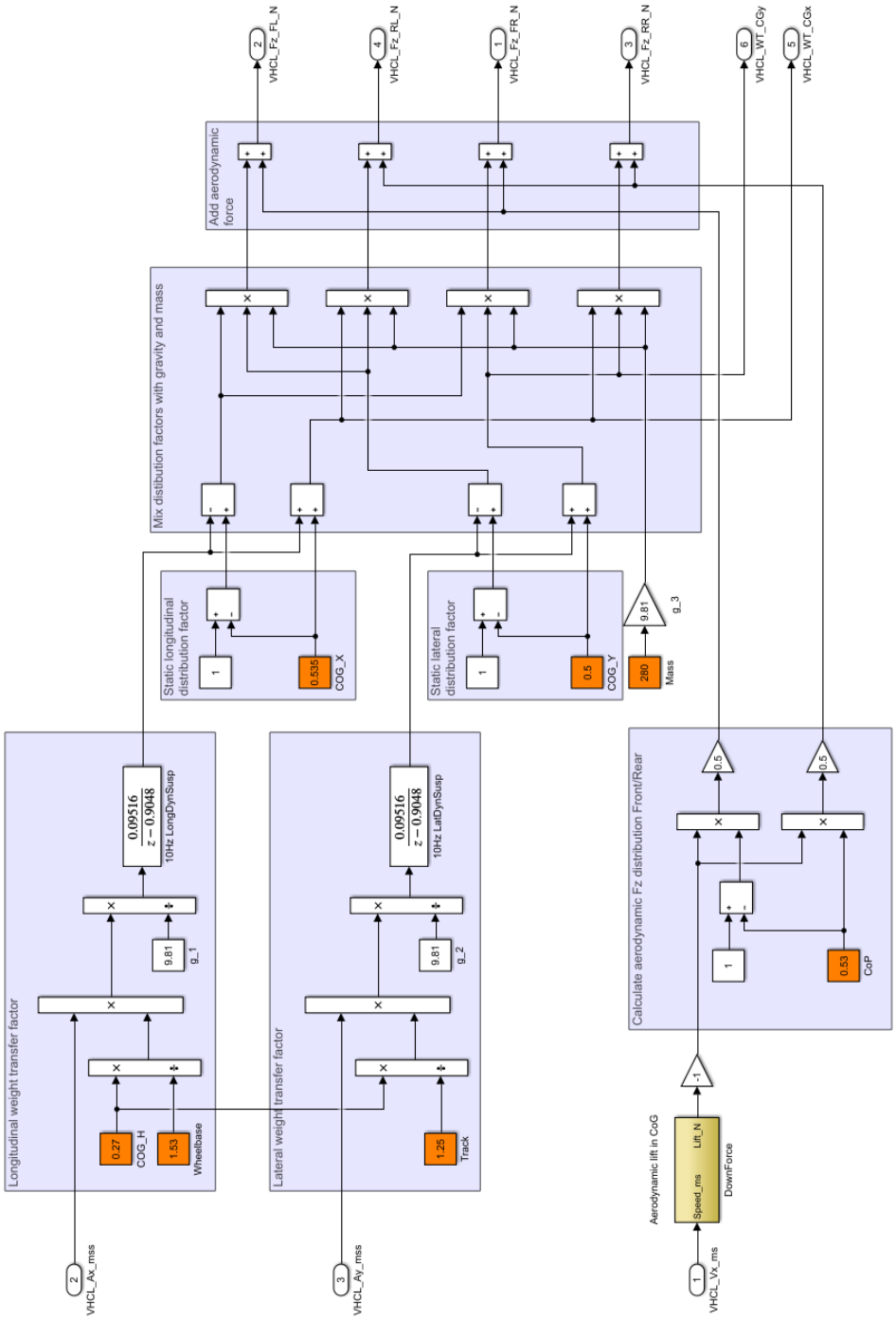

Figure A.9: Tire normal force estimator. Estimates the tire normal force using acceleration and estimated vehicle speed.

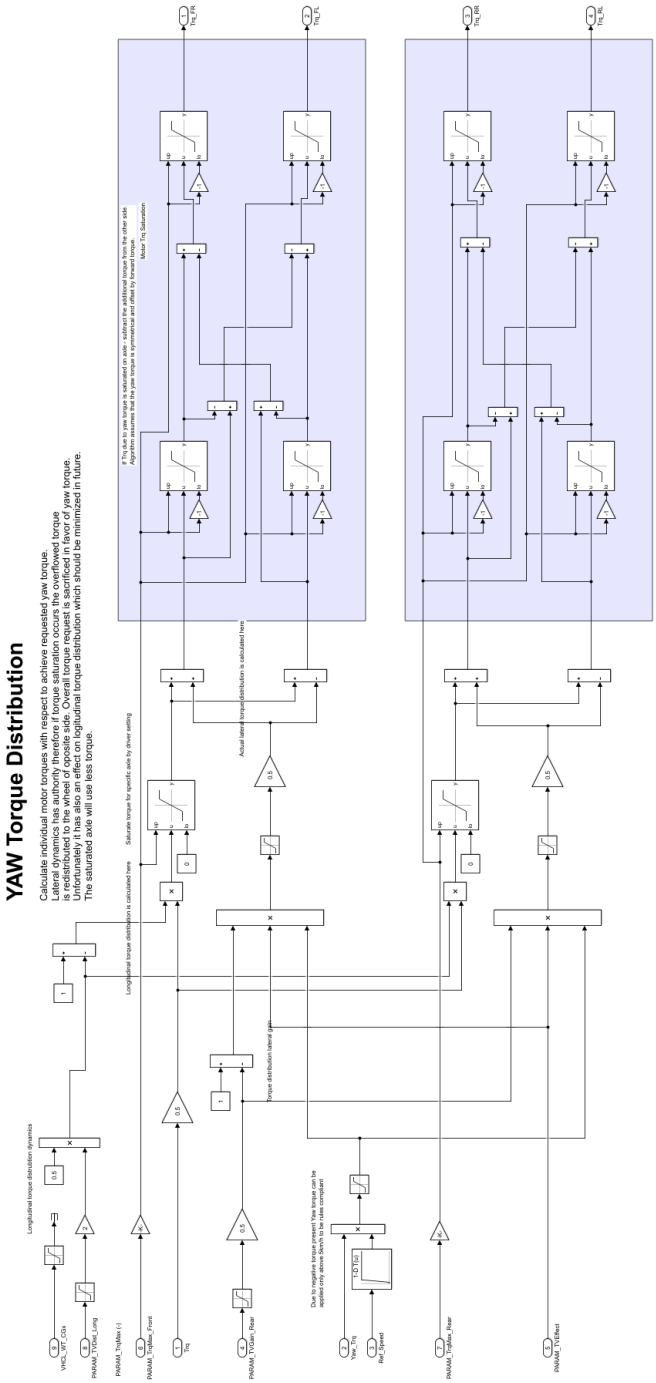

Figure A.10: VDCU torque distribution. Implementation of torque distribution algorithm that fulfills the torque and yaw torque demands.

Appendix B

Parameters

Description	Notation	Value
Vehicle mass	m	285 kg
Vehicle principal axis moment of inertia	I_z	120 kgm^2
Vehicle wheel base	w_b	1.54 m
Height of center of gravity	h	0.27 m
Longitudinal distance of front axle from center of gravity	a_1	0.72 m
Longitudinal distance of rear axle from center of gravity	a_2	0.82 m
Longitudinal distance of front axle from center of pressure	a_{CL1}	0.68 m
Longitudinal distance of rear axle from center of pressure	a_{CL2}	0.86 m
Lift coefficient of vehicle body related to center of pressure	C_L	-3.5
Aerodynamic reference area	S	1.19m^2
Air density	ρ	1.225 kgm^{-3}

Table B.1: Single track vehicle model parameters.

Description	Notation	Value
Tire dynamic radius	r	0.2
Tire vertical stiffness	k_v	80kNm^{-1}
Longitudinal shape factor	C_x	1.4
Longitudinal peak factor	D_x	1.4
Longitudinal stiffness factor	B_x	0.165
Longitudinal curvature factor	E_x	-1
Lateral shape factor	C_y	1.45
Lateral peak factor	D_y	1.4
Lateral stiffness factor	B_y	0.184
Lateral curvature factor	E_y	-0.3
Lateral self aligning factor	C_z	3.75
Lateral self aligning factor	D_z	-0.03
Lateral self aligning factor	B_z	0.11
Lateral self aligning factor	E_z	0.90

Table B.2: Pacejka '94 tire parameters used with single track model.

Appendix C

Content of encloused CD

```
./
├── Figures
└── DP_Laszlo.pdf
```